CHALMERS

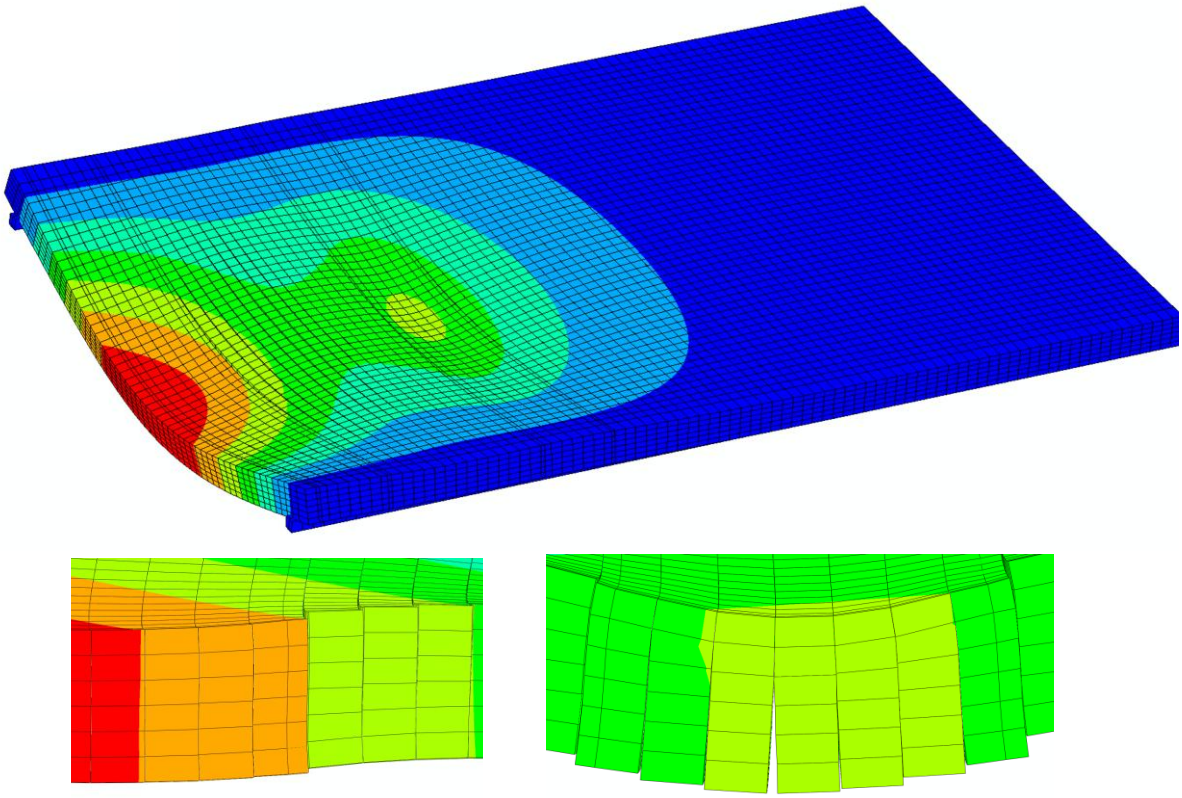

Finite Element Modelling of Local Interlaminar Slip in Stress-Laminated-Timber Bridges

Master's Thesis in the Master's programme Structural Engineering and Building Performance Design

JACOB HELLGREN
LUDWIG LUNDBERG

Department of Civil and Environmental Engineering
Division of Structural Engineering
Steel and Timber Structures
CHALMERS UNIVERSITY OF TECHNOLOGY
Göteborg, Sweden 2011

Master's Thesis 2011:13

MASTER'S THESIS 2011:13

Finite Element Modelling of Local Interlaminar Slip in Stress-Laminated-Timber Bridges

Master's Thesis in the *Master's programme Structural Engineering and Building Performance Design*

JACOB HELLGREN
LUDWIG LUNDBERG

Department of Civil and Environmental Engineering
Division of Structural Engineering
Steel and Timber Structures
CHALMERS UNIVERSITY OF TECHNOLOGY
Göteborg, Sweden 2011

Finite Element Modelling of Local Interlaminar Slip in Stress-Laminated-Timber Bridges
Master's Thesis in the Master's programme Structural Engineering and Building Performance Design
JACOB HELLGREN
LUDWIG LUNDBERG

Examensarbete 2011:13
Department of Civil and Environmental Engineering
Division of Structural Engineering
Steel and Timber Structures
Chalmers University of Technology
SE-412 96 Göteborg
Sweden
Telephone: + 46 (0)31-772 1000

Cover:
Deflection profile for a stress-laminated-timber deck consisting of 84 glue-laminated beams, subjected to an axle load placed at the left edge, with highlight of slip and gap between beams.

Chalmers Reproservice / Department of Civil and Environmental
Göteborg, Sweden

Finite Element Modelling of Local Interlaminar Slip in Stress-Laminated-Timber Bridges

Master's Thesis in the *Master's programme Structural Engineering and Building Performance Design*

JACOB HELLGREN
LUDWIG LUNDBERG
Department of Civil and Environmental Engineering
Division of Structural Engineering
Steel and Timber Structures
Chalmers University of Technology

ABSTRACT

Stress-laminated-timber decks are a common type of structure when building modern timber bridges. They are generally constructed of several glue-laminated timber beams placed side by side and pressed together with high strength steel rods. When designing stress-laminated-timber decks today it is difficult to utilize the full capacity of the structure due to lack of knowledge of the structural behaviour. Because of this, there is reason to believe that the stress-laminated-timber decks that are made today contain a large overcapacity, which is an economic disadvantage.

Today, linear elastic models are used to describe the behaviour of stress-laminated-timber decks. However, results from experimental test showed that the response may not be linear when applying loads until failure. Instead interlaminar slip between the beams will occur at high loads when the stresses overcome the resisting compressive stresses causing redistribution of forces. This slip is thus of great importance when trying to understand the behaviour of stress-laminated-timber decks.

The first aim of this thesis was to investigate and describe how to model frictional behaviour in the finite element software ABAQUS. This is done by creating a simple model and run several analyses with different friction and contact properties. With help of the knowledge gained in the first model a second model was created. The second model was used to validate that the approach of modelling friction in ABAQUS is consistent with experimental tests.

The second aim of the thesis was to investigate whether it is possible to create a model describing a stress-laminated-timber deck. This was performed in the third model, which corresponds to the stress-laminated-timber deck in the full-scale ultimate-load test performed by SP Trätek. The third model was also verified against the full-scale test.

The results from the models are in general good and important physical phenomena are captured in the analyses. However, it is shown that there are some factors which are difficult to determine and needs to be further studied. Overall, the outcome of this thesis can be seen as a pre-study for future finite element analyses of stress-laminated-timber decks.

Key words: Stress-laminated-timber deck, timber bridges, interlaminar slip, friction in ABAQUS, contact, FEM

Finit element-modellering av lokala glidningar mellan balkar i tvärspända broplattor av trä

Examensarbete inom *Masterprogrammet Structural Engineering and Building Performance Design*

JACOB HELLGREN
LUDWIG LUNDBERG
Institutionen för bygg- och miljöteknik
Avdelningen för konstruktionsteknik
Stål och träbyggnad
Chalmers tekniska högskola

SAMMANFATTNING

Tvärspända träplattor är en vanlig konstruktionstyp att använda vid byggnation av moderna träbroar. De utförs ofta med limträbalkar vilka placeras sida vid sida och pressas samman med tvärgående höghållfasta stålstag. På grund av bristande kunskap om hur tvärspända träplattor fungerar är det med dagens dimensioneringsmetoder svårt att utnyttja hela kapaciteten hos konstruktionen. Detta ger anledning att tro att de tvärspända plattbroar i trä som tillverkas idag är kraftigt överdimensionerade, vilket medför en ekonomisk nackdel gentemot andra brotyper.

Idag används linjärelastiska modeller för att beskriva beteendet hos tvärspända träplattor. Dock visar resultat från testförsök att responsen hos tvärspända träplattor inte är linjär när de belastas till brott. Istället uppstår glidning mellan balkarna vid stora laster när spänningarna mellan balkarna blir större än den mothållande tvärspänningen vilket förorsakar omfördelning av krafter i träplattan. Glidning mellan balkarna är således viktigt att beakta när man studerar responsen hos tvärspända träplattor.

Ett av målen med denna uppsats var att lära sig att modellera friktion i det finita element-programmet ABAQUS. Detta uppnås genom att skapa en enkel modell vilken sedan används till att utföra flera analyser med olika friktion- och kontaktegenskaper. Med hjälp av den kunskap som erhållits i den första modellen skapades en andra modell. Modellen användes för att säkerställa att tillvägagångsättet, vilket används för modellering av friktion i ABAQUS, överensstämmer med de tester som utförts.

Ett annat mål med uppsatsen var att undersöka huruvida det är möjligt att skapa en modell av en tvärspänd träplatta. Detta utfördes i den tredje modellen, som motsvarar den tvärspända träplatta som användes vid fullskaleförsök med belastning till brott utförda av SP Trätek. Den tredje modellen verifierades också mot fullskaleförsöket.

Resultaten som modellerna ger är generellt sett bra och fångar viktiga fysikaliska fenomen på ett trovärdigt sätt. Dock visar resultaten från samtliga analyser att det finns ett antal faktorer som är svåra att bestämma vilka också behöver studeras ytterligare. Totalt sett kan resultatet av denna uppsats ses som en förstudie för framtida finita element-analyser av tvärspända träplattor.

Nyckelord: Tvärspända träplattor, träbroar, friktion, lokal glidning mellan balkar, friktion i ABAQUS, kontakt, FEM

Contents

Preface

In this thesis, investigations of how to model frictional behaviour between beams in a stress-laminated-timber deck with use of the finite element program ABAQUS were performed. This was done by first creating a simple model which result was verified to the results from an experimental test performed by SP Trätek. The knowledge gained of how to model friction was applied on a larger model representing a stress-laminated-timber deck consisting of 84 beams.

The thesis was carried out from September 2010 to April 2011. The work is a part of the research project "Competitive timber bridges", and it was carried out at the Division of Structural Engineering, Steel and Timber Structures, Chalmers University of Technology. The research project is financed as a part of VINNOVA's trade research programme with the two timber bridge manufactures, Moelven Töreboda AB and Martinsons Träbroar AB as the main financiers. The project was carried out with Dr. Morgan Johansson at REINTERSEN Sverige AB and PhD-student Kristoffer Karlsson at Chalmers as supervisors and Professor Robert Kliger as examiner.

We would like to thank our supervisors Morgan Johansson and Kristoffer Karlsson for all the effort and time they put down during the whole process with this thesis. Their knowledge has been essential for us in our learning process and work with this thesis. We would also thank our examiner Professor Robert Kliger for his opinions and also our opponent Johan Eriksson for his comments and support.

Göteborg, April 2011

Jacob Hellgren

Ludwig Lundberg

Notations

Roman upper case letters

A	Area
E	Modulus of elasticity
E_L	E-modulus longitudinal
E_R	E-modulus radial
E_T	E-modulus tangential
F_f	Frictional force
G	Elastic slip stiffness
G	Shear modulus
G_{LR}	Shear modulus longitudinal-radial
G_{LT}	Shear modulus longitudinal-tangential
G_{RT}	Shear modulus radial-tangential
L	Length
I	Moment of inertia
M	Bending moment
N	Pre-stressing force
N	Normal force
P	Load
S	First moment of area
V	Shear force
W	Bending resistance

Roman lower case letters

b	Width of one beam
l	Length of timber beam
q	Distributed load
u	Vertical deflection
w	Width of timber deck

Greek letters

μ	Frictional coefficient [my]
μ_2	Frictional coefficient dynamic
μ_s	Frictional coefficient static
μ_k	Frictional coefficient kinetic
$\mu_{parallel}$	Frictional coefficient parallel the fibres
$\mu_{perpendicular}$	Frictional coefficient perpendicular the fibres
γ	Elastic slip [gamma]
γ'	Slip rate
γ'_{eq}	Equivalent slip rate
σ_i	Bending stress [sigma]
τ	Shear stress [tau]
ν	Poisson's coefficient [ny]
ν_{LR}	Poisson's coefficient longitudinal-radial
ν_{LT}	Poisson's coefficient longitudinal-tangential
ν_{RT}	Poisson's coefficient radial-tangential

1 Introduction

1.1 Background

When building timber bridges a suitable way is to build it as an orthotropic plate with good strength and sustainability. This plate is generally made up of several glue-laminated timber beams placed side by side and pressed together with high strength steel rods, thus creating a stress-laminated-timber deck. When designing stress-laminated-timber decks today it is difficult to utilize the full capacity of the structure due to lack of knowledge of the structural behaviour. Because of this, there is reason to believe that the stress-laminated-timber decks that are made today contain a large overcapacity, which is an economic disadvantage.

Today, linear elastic models are used to describe the behaviour of stress-laminated-timber decks. However, results from experimental test showed that the response of such timber plates may not be linear when applying loads until failure. Instead interlaminar slip between the beams will occur when the loads reach certain level and the stresses overcome the resisting compressive stresses. When slipping occurs between the beams, due to shear forces or bending moment, deformations and stresses will be redistributed. This slip is thus of great importance when trying to understand the behaviour of stress-laminated-timber decks.

1.2 Aim of the study

The main aim of this thesis is to by using the commercial finite element program ABAQUS, create a reliable finite element model which describes the non-linear behaviour that occurs in stress-laminated-timber decks. The model shall be verified against results from experimental tests. A central part of the process will be to understand and document how to model the frictional behaviour between the timber lamellas when the load increases until failure.

The model shall be used to improve the understanding of stress-laminated-timber decks and thereby be able to use the material more effective when designing timber bridges in the ultimate limit state.

The documentation of the work and the final models shall also be used as a pre-study to forthcoming studies and finite element analyses of the subject.

1.3 Limitations

This thesis focuses on how to model a specific part of a stress-laminated-timber deck by help of the finite element program ABAQUS. Hence an entire timber bridge is not analysed, i.e. only a simplified superstructure is analysed. The friction which occur when the part is exposed to shear forces as well as bending and twisting moment is examined in the analysis with help of the friction models available in ABAQUS.

1.4 Method

A literature study of the subject has been made which includes general information, which is known up to today, concerning stress-laminated-timber decks as for instance

the structural behaviour. The focus has been on the frictional behaviour between the lamellas and how to model that properly in ABAQUS.

The modelling started with creating a very simple model that consisted of a small body which was moved on a plane. The model was subjected to a load perpendicular the plane and thus a frictional force was created between the body and the plane. When this model was verified and worked properly, a new slightly more advanced model was created that consisted of two bodies in contact. This model was verified against results from an experimental test, with regards to friction, to determine that the frictional behaviour worked in a similar, and proper, way.

By extensions of that model it was possible to model a larger number of beams, representing a stress-laminated-timber deck.

1.5 Outline

1. Introduction
A brief background, purpose and method for the thesis are presented in this part.

2. Literature study
The literature study is presented which includes a brief part about the history of stress-laminated-timber decks, different bridge types which uses stress-laminated-timber deck and also the structural behaviour is described. A presentation of the different frictional models that exist in ABAQUS and their properties are carried out.

3. Experimental tests by SP Trätek
Experimental tests, performed by SP Trätek, are presented. How the tests were performed and the results achieved are described.

4. Model 1 – Box on a plane
The first model that was created and analysed with the finite element method in this thesis is presented. This model was the first attempt to learn how to model friction in ABAQUS.

5. Model 2 – Frictional test by SP Trätek
The second model created in this thesis is presented. The model was verified against experimental tests that have been performed by SP Trätek.

6. Model 3 – Full-scale test by SP Trätek
A stress-laminated-timber deck was modelled in this chapter with the same dimensions and properties as the full-scale test that have been performed by SP Trätek.

7. Discussion
The discussion includes comments about the different models. It also threats important factors for modelling of frictional behaviour.

8. Conclusion
The most important conclusions are submitted and described here.

9. References
The references that have been used for this thesis is listed in an alphabetic order.

2 Literature study

2.1 Timber bridges

This section includes a brief description of different types of timber bridge, which are most common in the modern timber bridge industry. The most common timber bridge built today in Sweden, is some sort of stress-laminated-timber bridge, Martinsons (2010). This type of bridge can be divided into three different subtypes depending on their cross-section which will be presented further in Section 2.2.

All three types of stress-laminated-timber bridges can be combined with different primary load carrying systems, related to various bridge span. One such a system, for example, is the three hinged arch bridge as shown in Figure 2.1. Here the bridge deck consists of glulam beams that are pre-stressed in the transverse direction. The deck is carried by transversal beams that are supported by hangers connected to the arch.

Figure 2.1 Three hinged arch bridge over E18 in Hägernäs, Moelven Töreboda AB (2010).

Another type of primary load carrying system is the king post truss. An example of a king post truss bridge combined with a stress-laminated deck is shown in Figure 2.2. In this bridge structure the stress-laminated-timber deck is supported in the middle of a transverse beam. The beam is connected with hangers to the top of the structure, i.e. where the inclined glue-laminated beams are connected to each other. The forces are then transmitted to the abutments. There can also be tension bars between the ends of the inclined glue-laminated beams, see Figure 2.2 that help the abutment to resist the horizontal forces.

Figure 2.2 A king post bridge with a stress-laminated deck in Umeå, Träguiden (2010).

2.2 Stress-laminated-timber bridge decks

2.2.1 History

Stress-laminated-timber decks was first utilized in Canada, in the 1970`s when engineers developed a technique to repair old nail-laminated timber bridge decks. The engineers put transversal pre-stressing steel rods above and below the longitudinal nail-laminated timber deck as is illustrated in Figure 2.3. The technique worked well and extended the life of the timber bridge significantly. Since this technique was promising, more studies was carried out, that finally ended up in a design procedure for stress laminate timber decks at the end of the 1970´s. The first stress-laminated-timber bridge deck, that was constructed using this design procedure, was erected in 1981 at Fox Lake Road at the city Espanola in the state Ontario, Canada, Kalbitzer (1999).

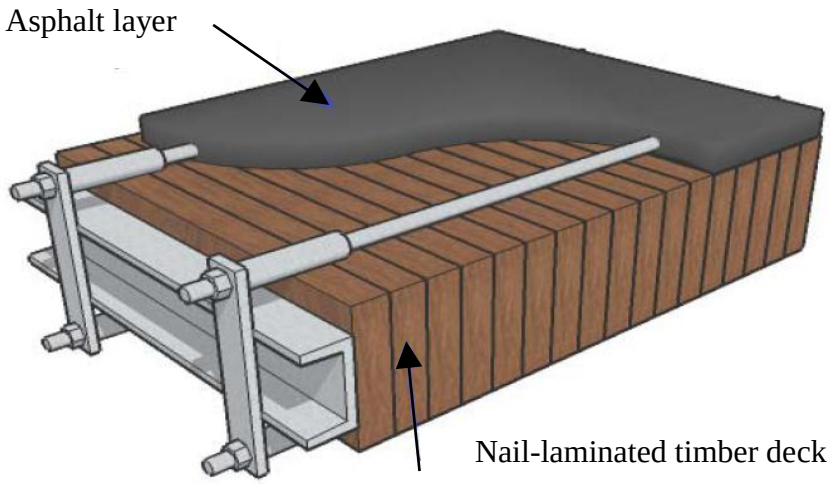

Figure 2.3 A schematic illustration of the repairing method for nail-laminated timber deck according to Andersson and Bergendahl (2009).

In the beginning of the 1980´s this technique were brought to the United States of America and the Forest Product Laboratory of the United States Department of Agriculture started to evaluate and test the Canadian system. The result was a design procedure for United State of America and their first stress-laminated-timber bridge were built in 1987 at Cross River Bridge in Cook County, Minnesota.

The first time this technique was used in Europe was 1985 when the bridge Dörfilbrücke in Switzerland needed to be exchanged. In Sweden two road bridges in Skellefteå were built in 1994, see picture Figure 2.4. The bridges were used for heavy road traffic which was new in Sweden for stress-laminated bridges, Kalbitzer (1999).

Figure 2.4 Arch bridge in Skellefteå, built as a road bridge in 1994, Träguiden (2010).

2.2.2 Stress-laminated-timber bridge

A stress-laminated-timber bridge in Sweden normally consists of glulam beams made out of Norway Spruce. These beams are pre-stressed together in the transverse direction and form the shape of a slab as shown in Figure 2.5. This bridge type is the main object for the analysis in this thesis, and it will be further investigated in the following sections.

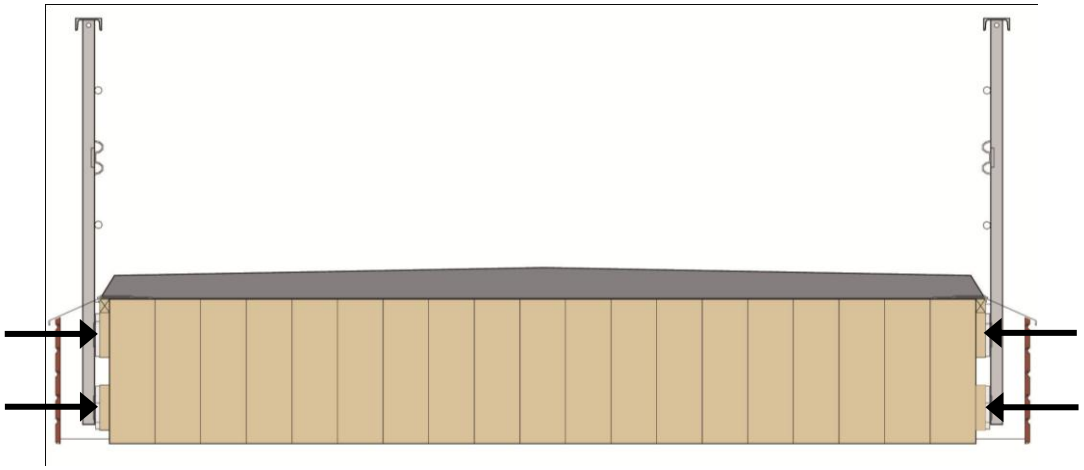

Figure 2.5 Cross-section of a stress-laminated-timber bridge with placement of pre-stressing force indicated, Träbroguiden (2010).

2.2.3 Box bridge

The box bridge consists of glulam beams that are placed on the edge in vertical direction and between them other glulam beams are placed on the edge in horizontal direction as showed in Figure 2.6. The pre-stressing steel rod is placed through the top and bottom of the box in the transversal direction.

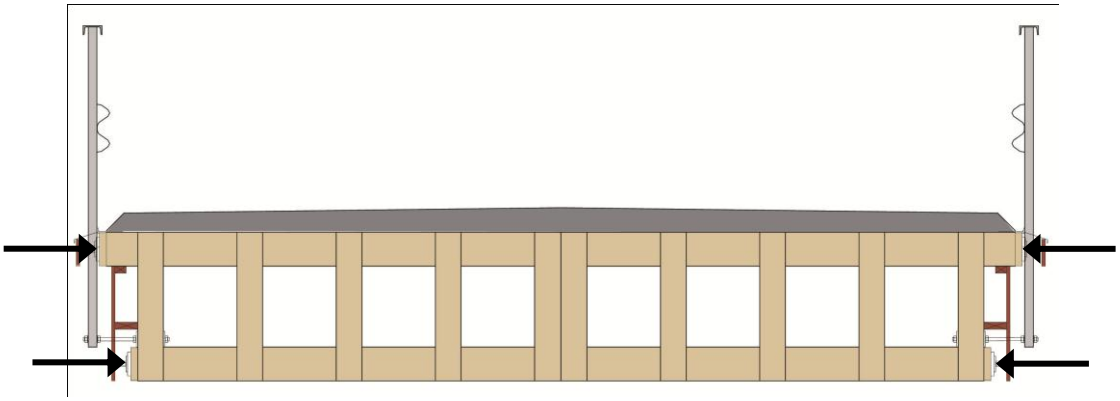

Figure 2.6 Cross-section of a box bridge with placement of pre-stressing force indicated, Träbroguiden (2010).

2.2.4 T-beam bridge

The T-beam bridge is also made up of glulam beams. Here the pre-stress rods are placed in the top part of the cross-section see Figure 2.7, which then form a slab. Longitudinal beams are placed into the slab, which increase the longitudinal stiffness of the cross-section.

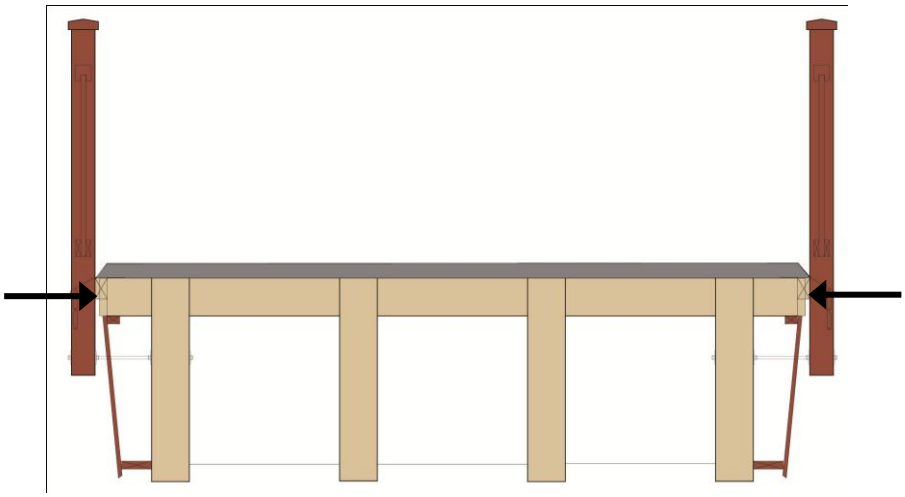

Figure 2.7 *Cross-section of a T-beam bridge with placement of pre-stressing force indicated, Träbroguiden (2010).*

2.2.5 Construction technique

A stress-laminated-timber deck can be made up of glulam beams, solid timber beams or laminated veneers lumber beams that are placed beside each other to form a deck. To make the deck act as an orthotropic slab the laminates are pre-stressed in the transversal direction by steel rods. The steel rods are placed through predrilled holes in the lamellas, see Figure 2.8, which is applied for construction of new bridges. It is also possible to put the steel rods above and below the lamellas, see Figure 2.9, which is common for rehabilitation of old bridges, Kalbitzer (1999).

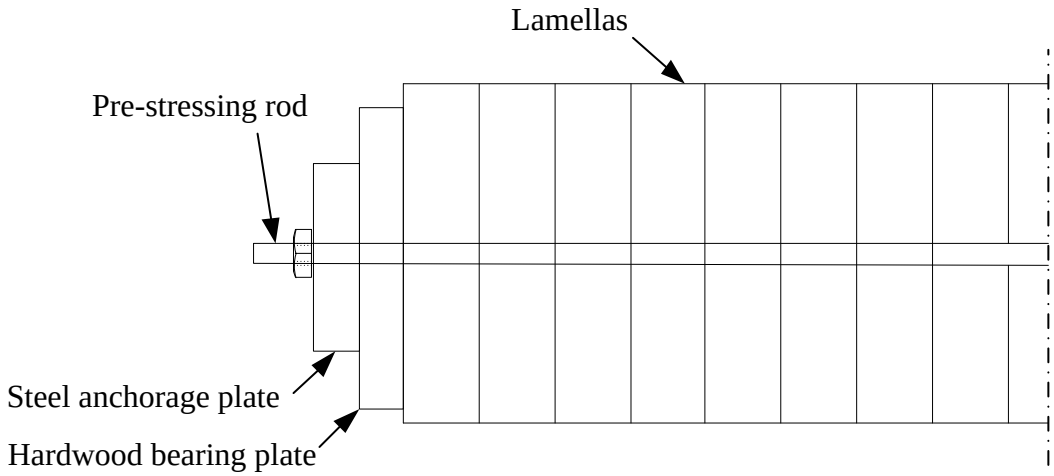

Figure 2.8 *Internal post-tension. The steel rods are placed through predrilled holes in the lamellas, based on Kalbitzer (1999).*

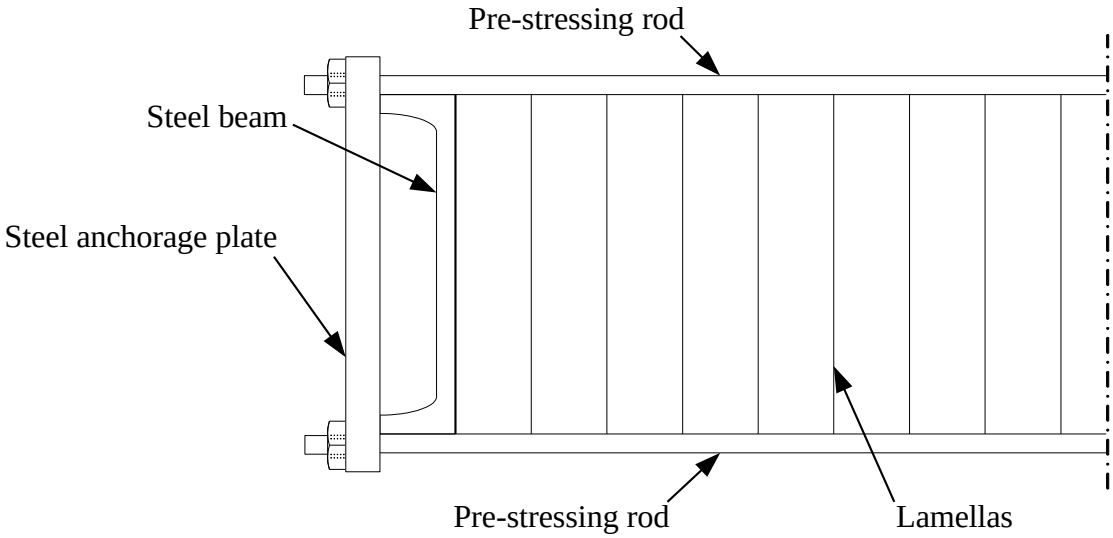

Figure 2.9 External post-tension. The steel rods are placed above and below the deck, based on Kalbitzer 1999.

The pre-stressing force creates a resisting friction force between the lamellas that make the lamellas interact with each other and the global response becomes similar to an orthotropic plate. In Figure 2.10 the response of a deck with and without pre-stressing is schematically compared. With pre-stressing, the load which in this case is a point load is distributed due to interaction between the lamellas on to several lamellas. This differs from the deck without pre-stressing where the load is distributed on just one lamella, i.e. no interaction between the lamella occurs.

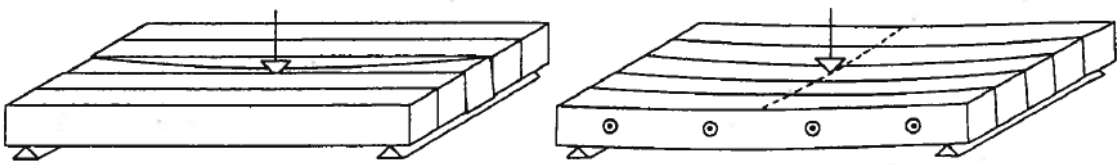

Figure 2.10 Different action between laminate deck without pre-stressing and with pre-stressing according to Kalbitzer (1999).

The deck can be placed between supports as simply supported or as continuously over the supports. For long bridges, with continuous deck, so called butt joints can be used to increase the length of the lamellas. In butt joint the ends of two lamellas are placed against each other, see Figure 2.11. Because of the butt joints are displaced against each other in the longitudinal direction of the timber deck, there is no limit for the maximum length of the deck, Pousette (2010).

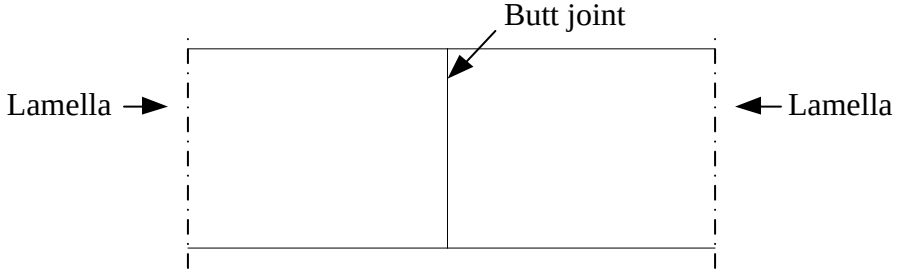

Figure 2.11 Elevation of a butt joint in a stress-laminated-timber deck.

2.2.6 Purposes of pre-stressing

When a stress-laminated-timber deck is subjected to a load one issue is to have enough pre-stressing force to gain good friction between the lamellas to prevent interlaminar slipping, see Figure 2.12. Another issue is to have enough pre-stressing force to prevent opening between the lamellas in the bottom of the deck, see Figure 2.13. Vertical interlaminar slipping is caused by transversal shear while opening between the lamellas in the bottom of the deck is caused by transversal bending. To prevent this behaviour the pre-stressing force need to be kept at a sufficient high level, Kalbitzer (1999).

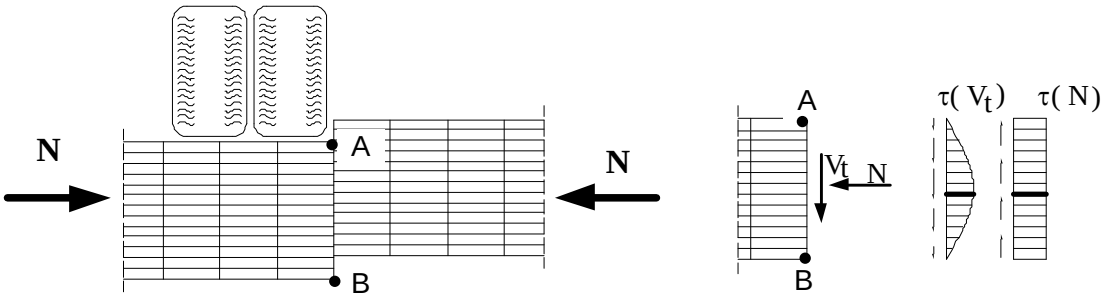

Figure 2.12 Interlaminar slip due to transversal shear.

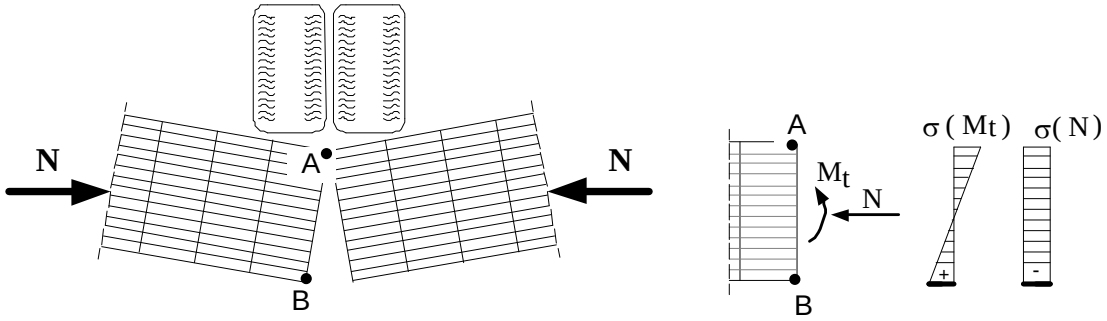

Figure 2.13 Opening between the lamellas in the bottom of the deck caused by transversal bending.

2.3 Glue-laminated timber

The most common type of timber used when manufacturing glue-laminated timber (glulam) in Sweden is Norway spruce (*Picea abies*). Glulam consists of studs, normally called lamellas, which are glued together with the grain parallel to the length, see Figure 2.14. The minimum number of lamellas in Sweden for it to be named glulam is four. If it is less than four lamellas it is not called glulam, Träguiden (2010). The thickness of the lamellas is between 25 and 50 mm, FPL Wood Handbook (2010). The lamellas are glued together with moisture content of 12% and with an adhesive that have good resistance.

The shape of the beams can be straight or curved and the size of the beams is limited by the machines that manufacture them. Today in Scandinavia it is limited to 215 mm in width and 2000 mm in height. The beams can consist of either lamellas with the same strength in all layers or lamellas with different strength. It can be useful to put

lamellas with higher strength in the layer close to top and bottom of the beam and use lamellas with less strength in the middle. These beams are called combined glulam with index c.

Figure 2.14 Glulam beams that consist of lamellas with different measures, Träguiden (2010).

2.3.1 Material properties

This part contains a compilation of data regarding material properties, Persson (2000), Formolo and Granström (2007), Fortino and Toratti (2008), Pousette (2001), see Table 2.1. The material properties that are treated in this section are Young's modulus, Shear modulus and Poisson's ratio, all in three directions. These are the material properties that are of interest for the type of models that is used in this thesis.

Table 2.1 Compilation of different material properties of glulam.

Parameter	A	B	C	D
E_L [MPa]	13500-16700	11750-13000	11500-12500	10000-11000
E_R [MPa]	700-900	590-700	550-650	650-750
E_T [MPa]	400-650	260-360	550-650	400-450
G_{LR} [MPa]	620-720	560-600	600-750	300-350
G_{LT} [MPa]	500-850	300-400	600-750	170-220
G_{RT} [MPa]	30-40	25-30	30-50	30-40
ν_{LR} [-]	0.02-0.03	0.01-0.02	0.03-0.05	0.02-0.03
ν_{LT} [-]	0.01-0.02	0.01-0.02	0.01-0.04	0.02-0.03
ν_{RT} [-]	0.25-0.35	0.20-0.25	0.40-0.60	0.25-0.35

A= Persson (2000).

B= Formolo and Granström (2007).

Both A and B is for glue-laminated timber in class L40 with 12% moisture content.

C= Fortino and Toratti (2008), Norway spruce 12% moisture content.

D= Pousette (2001), Norway spruce 12% moisture content

2.3.2 Friction coefficient

This thesis mainly treats static and kinetic friction coefficients for planned glulam made out of spruce. These coefficients are affected by three principal properties which are the fibre direction, the surface roughness and the moisture content.

- Fibre directions

  Because this thesis is about timber decks that consist of glulam beams that are pre-stressed together causing interlaminar friction, there is only main interest to study the friction coefficients in two directions, i.e. the longitudinal and the transverse direction. The friction coefficient is normally higher in the transverse fibre direction compared with the longitudinal fibre direction. It is due to the interlocking that occur between the fibres when two wood surfaces interacts with each other, Kalbitzer (1999).

- Surface roughness

  There are two different surfaces that are of interest concerning surface roughness in wood: sawn or planed, Kalbitzer (1999). Sawn wood has often higher friction coefficient, but this thesis only include planed wood.

- Moisture content

  The friction coefficient increase when the moisture content increases from oven dry to fibre saturation. If the moisture content is increased from fibre saturation until the surface start to feel wet, the friction coefficient is constant. The friction coefficient starts to decrease when the surface are flooded with water. These phenomena concern both static and kinetic coefficients.

  Concerning kinetic friction, speed of movement between two surfaces is an affecting property. When moisture content is less than 20% the kinetic friction coefficient varies slightly with regards to speed, however when the moisture content is larger the kinetic friction coefficient depends more on moisture, it decreases significantly when the speed of movement between the surfaces increases, FPL Wood handbook (2010).

2.4 Friction modelling in ABAQUS

2.4.1 Contact

Contact between two surfaces can be modelled in three different ways in ABAQUS. One way is to use contact elements, whereas there are several different contact elements with different properties for different contact models.

Another option is to use contact pairs. The contact pair is given different properties depending on which type of behaviour to be modelled. The contact behaviour could be defined in both in the tangential and the normal direction.

The last option is called general contact. The approach for this option is approximately the same as for contact pairs except that the algorithm used is not the same. Another difference is that contact properties and surface attributes are independent of each other for general contact. This makes general contact option more flexible than contact pair option.

When using contact pair or general contact one of the two surfaces has to be assigned as a master surface and the other have to be slave surface. The master surface's nodes control the motion of the slave surface's nodes.

2.4.2 Coulomb friction

In ABAQUS the friction model used is based on the Coulomb friction model as shown inFigure 2.15. This model can be modified in different ways. The basic of the Coulomb friction model is the approximation that the force F needed to move the box over a surface, depends on the normal force N. F is independent of the contact area between the surfaces, since the two surfaces are approximated to be in contact over the entire area.

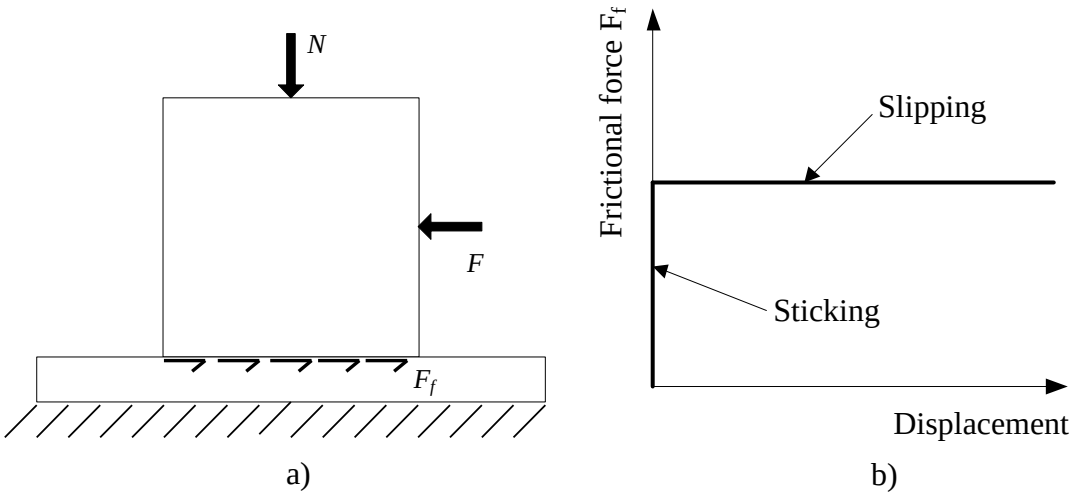

Figure 2.15 (a) Basic Coulomb friction model and (b) ideal Coulomb friction curve.

The frictional coefficient, μ is a scalar describing the ratio of friction between the two surfaces. The value of μ is between 0 and 1. Values of μ can be found in literature whereas they mostly are determined from experimental tests.

The frictional force, F_f that occurs at the interface of the two parts depends on the frictional coefficient, μ. The relationship between the acting normal force, the frictional coefficient and the resulting frictional force is showed in Equation 2.1 and 2.2.

$$F_f = \mu \cdot N \tag{2.1}$$

$$F = F_f \tag{2.2}$$

Different formulations of friction can be used in ABAQUS as interaction properties. These formulations are stated below and briefly presented in following sections.

- Penalty friction
- Static kinetic exponential decay
- Lagrange multiplier
- Rough friction
- User defined friction

The Coulomb friction model used in ABAQUS is extended to fit different purposes. For instance it is possible to put a limit on the allowable shear force, which can be useful when the model is exposed for a normal force that exceeds the compression capacity of the material. It is also possibility to define a "secant" friction coefficient which is useful when the friction have a non-linear behaviour.

2.4.3 Penalty friction formulation in ABAQUS

By default frictional constraints are enforced with the penalty friction formulation in ABAQUS. The penalty formulation is a stiffness imposed formulation of friction that permits some relative motion, i.e. elastic slip, of the actual surfaces when they should remain sticking.

The elastic slip is an important setting as it affects the frictional behaviour, before the slipping phase occurs, in a large extent. The elastic slip is defined as the distance where the slipping phase is reached or similar, how large the elastic movement is during the sticking phase, see Figure 2.16.

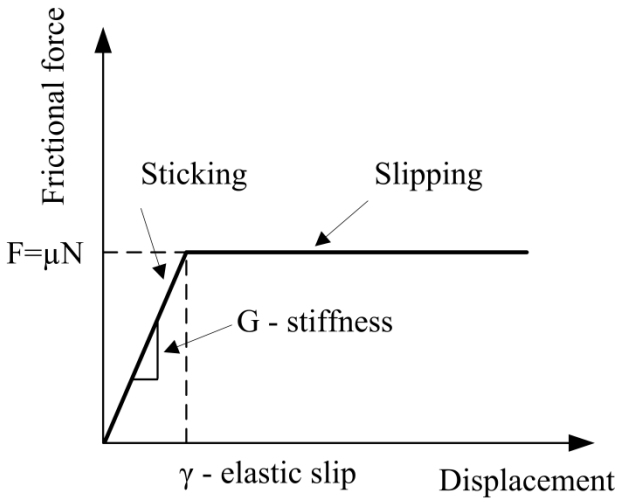

Figure 2.16 A general friction curve with penalty formulation based on ABAQUS analysis user´s manual 6.9 (2009).

The stiffness of the inclined curve, *G*, is defined as in Equation 2.3. A small elastic slip will increase the inclination of the curve and a larger value will decrease the inclination.

$$G = \frac{\mu \cdot N}{\gamma} \qquad \text{where } \gamma \text{ is the elastic slip} \tag{2.3}$$

On a physical level the elastic slip can be assumed to correspond to the elastic displacements in the surface roughness. To determine correct elastic slip, for an actual material, can difficult and even a bit arbitrary. However, this is a parameter which is possible to be adjusted to real material parameters to describe the real behaviour of the slip.

The elastic slip can be entered as fraction of the element length or as an absolute distance. By default the elastic slip is defined as 0.5% of the average length of all contact surface elements in the model, hence it is dependent of the element size. However, when defined as an absolute distance the elastic slip is not dependent on the element size.

When using a large elastic slip the computational time is improved, but with less solution accuracy. This is due to the fact that there is a greater relative motion of the surfaces when they should be in the sticking phase. To improve the solution accuracy, a small elastic slip should be used, ABAQUS analysis user's manual 6.9 (2009).

By default the penalty friction formulation use isotropic frictional properties, however there is a possibility to model with anisotropic friction properties as well. When using anisotropic friction in ABAQUS, the input consists of two different friction coefficients, one for each direction of the surface. The critical shear force i.e.

frictional force, for the two directions, forms an ellipse region which is showed in Figure 2.17. The size of this region depends on the contact force between the parts. The slip appears in the direction of the normal to the critical shear stress surface, ABAQUS analysis user's manual 6.9 (2009).

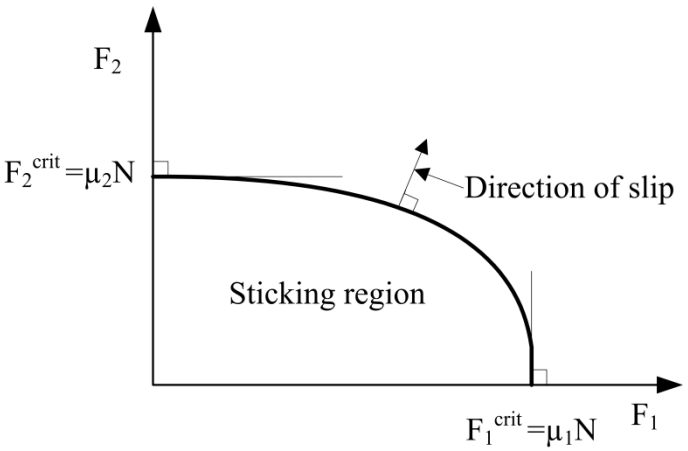

Figure 2.17 Critical shear force surface for anisotropic friction according to ABAQUS analysis user´s manual 6.9 (2009), where u_1, u_2, F_i and N_i as in Figure 2.15.

2.4.4 Static kinetic exponential decay

An extension of the penalty frictional formulation is the static kinetic exponential decay formulation. This formulation of friction also uses an elastic slip value as in the penalty formulation, but it has the possibility to use different coefficients for static friction and kinetic friction. It requires a coefficient for the decay that describes the change from static state to kinetic state. In Figure 2.18 the expression for the static kinetic exponential decay formulation is described, ABAQUS analysis user´s manual 6.9 (2009).

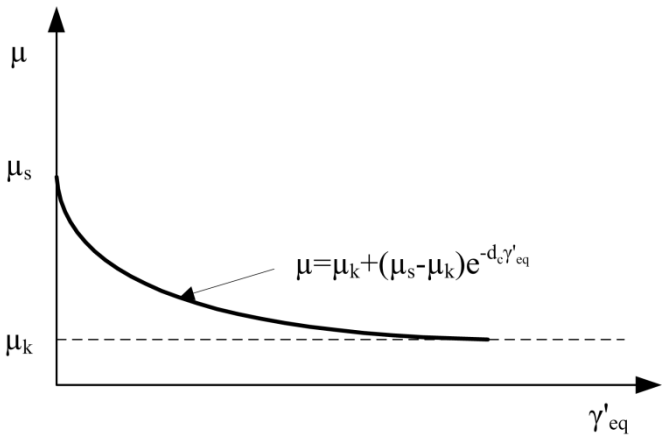

Figure 2.18 Static kinetic exponential decay formulation where d_c is the decay coefficient and γ'_{eq} is the equivalent slip rate according to ABAQUS theory manual 6.9 (2009).

It is also possible to choose an option called test data, see Figure 2.19, in the static kinetic formulation. Here the input consists of three different frictional coefficients for different slip rates. Slip rate is the time derivative of the slip, see Equation 2.4, i.e. it describes how fast slip occurs.

$$\gamma' = \frac{d\gamma}{dt} \qquad \text{where } \gamma \text{ is the slip} \tag{2.4}$$

The first input is a static frictional coefficient, μ_1, when the slip rate is zero. The second is a dynamic frictional coefficient, μ_2, which appears at a certain slip rate and finally a kinetic frictional coefficient, μ_3, for infinite slip ratio. Unlike the penalty friction formulation this formulation is only available for isotropic materials which may not be good for the further work in this thesis.

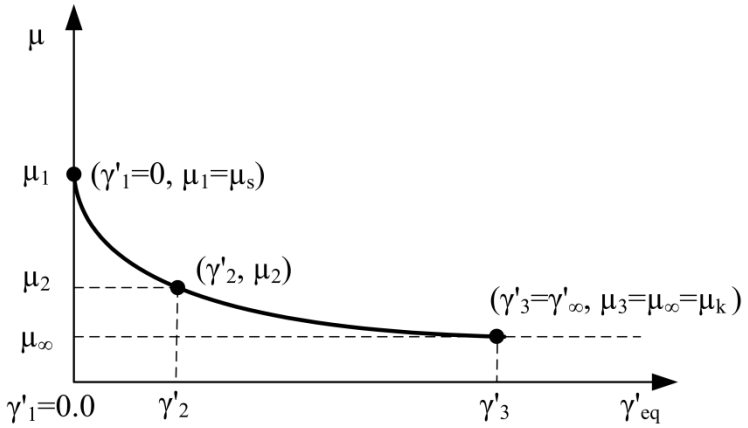

Figure 2.19 Test data formulation according to ABAQUS theory manual 6.9 (2009).

2.4.5 Lagrange multiplier formulation

Lagrange multiplier formulation set the elastic slip value to zero. The consequence of this is that the friction gets an ideal plastic behaviour. This formulation can have difficulties to convergence in areas where contact condition change, it is also time consuming when running the analysis. The advantages of using this formulation are that it gives an exact value of the slip, ABAQUS theory manual 6.9 (2009).

2.4.6 Rough friction

Rough friction is a formulation that works together with the Lagrange multiplier method. As long as the surfaces are in contact the friction coefficient is infinite large, hence no slip will occur. When rough friction formulation is used together with the restriction, that after contact the surfaces would not be able to separate, the model act as a homogenous solid and no relative motion will occur, ABAQUS theory manual 6.9 (2009).

2.4.7 User defined friction

If none of the mentioned formulations applies there is also a possibility to formulate a user defined friction. In both the penalty and Lagrange multiplier method formulation, it is possible to make the friction dependent of slip rate, contact-pressure and temperature data, ABAQUS theory manual 6.9 (2009).

2.5 Finite element modelling

2.5.1 Element type

ABAQUS and finite element modelling in general is performed by using different element types. Some of the most common type of element groups is

- Continuum (solid) elements
- Shell elements
- Beam element
- Truss element

This thesis only includes solid elements with 3 degrees of freedom per node and reduced integration.

Figure 2.20 a) shows an 8-node linear brick element, i.e. C3D8R, which refers to the group of element called first-order elements. They use a linear interpolation in each direction. Figure 2.20 b) illustrates a 20-node quadratic brick element, i.e. C3D20R, The element use a quadratic interpolation and belongs to the group called second order elements, ABAQUS analysis user´s manual 6.9 (2009).

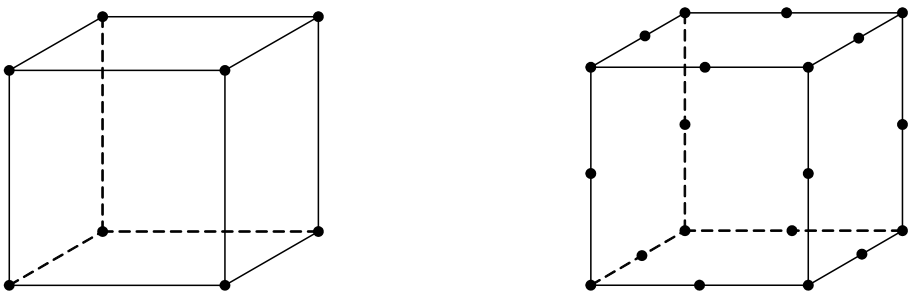

a) b)

Figure 2.20 In (a) a C3D8R element is showed and in (b) a C3D20R(S), ABAQUS analysis user´s manual 6.9 (2009).

Second order elements have problems with the contact algorithm. The reason to this is a miss balance between the compression and tension forces inside an element, see Figure 2.21. This leads to problem with convergence and errors in the result. It is more reliable to use first order elements in contact analyses, because they do not have such problems with the contact algorithms.

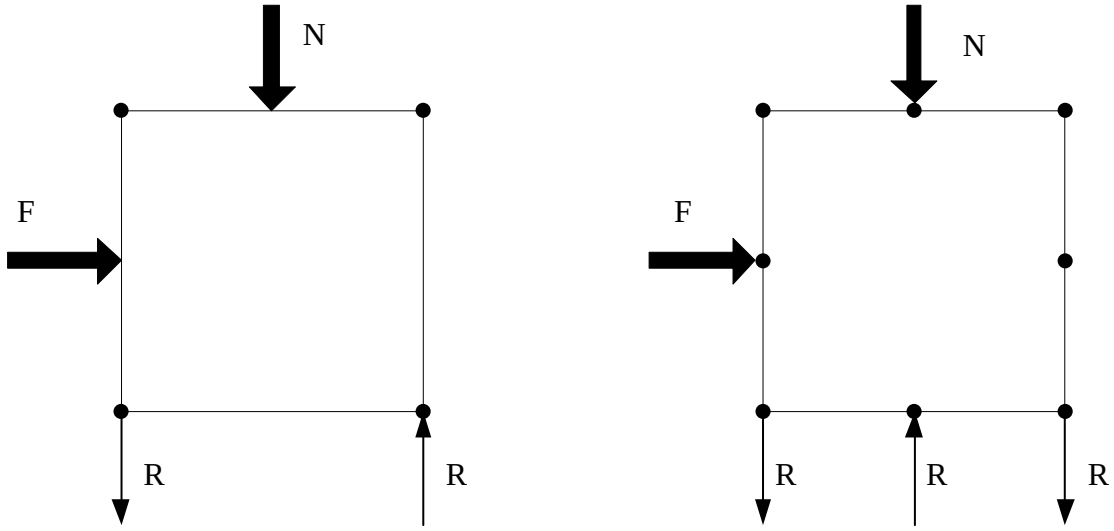

Figure 2.21 Difference between force balance in an 8-node and a 20-node element.

2.5.2 Load application

The load can be introduced to a model by prescribing a deformation for a certain time. For instance, the displacement of a body next to another can be set to move 1 mm in a defined direction over a time of 2 seconds. This movement between the bodies results in a force between them. This is called deformation controlled load application and it is very useful to describe the load in this manner when the response of the system is nonlinear, see Figure 2.22. A load can be applied instantaneous i.e. in the beginning of an analysis step. The load can also be applied step by step over a defined time which is called ramped load application.

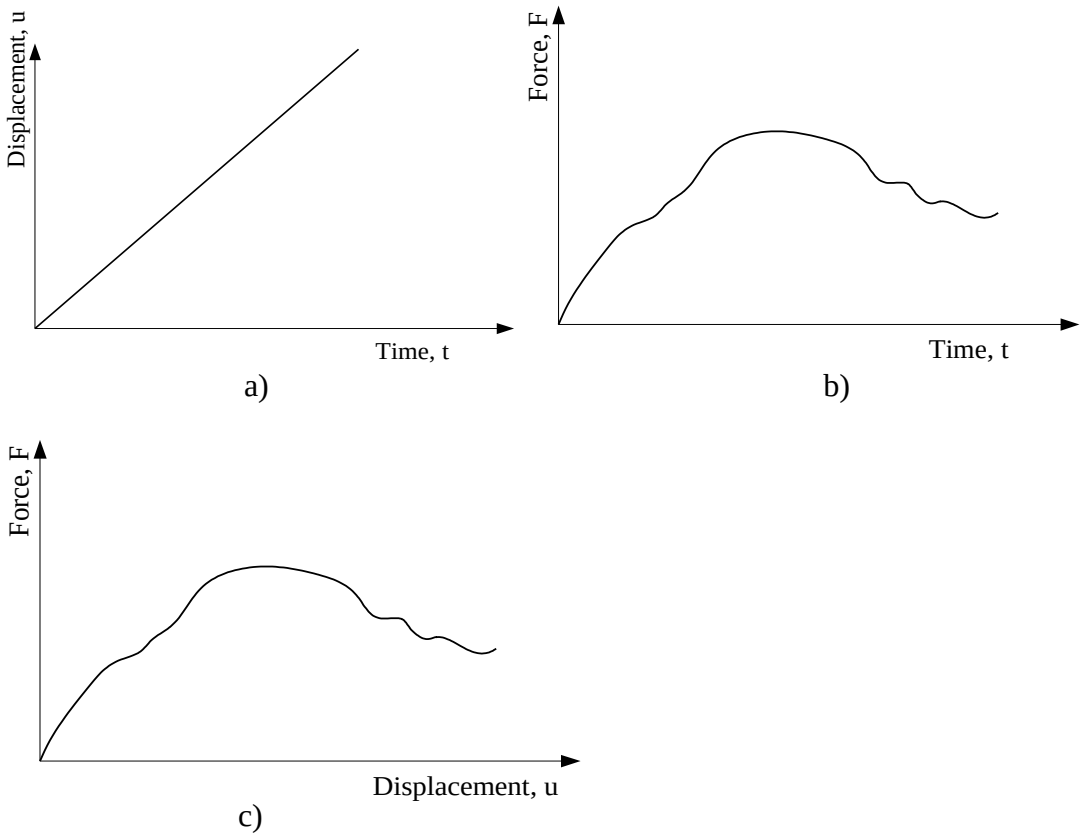

Figure 2.22 a) Displacement changes according to time, b) Force varies during time c) Combination of a and b.

2.5.3 Iteration method

In ABAQUS there are three different iteration methods to choose from.

- Full Newton
- Quasi Newton (BFGS)
- Contact iteration

The analyses for this thesis are made with the Full Newton and thereby this thesis only describes the Full Newton iteration method.

2.5.4 Time step

Every step in an analysis is divided into increments, which size is prescribed by the user. In each increment the goal is to find equilibrium i.e. to follow the non-linear path, see Figure 2.23 a). Inside an increment there can be several iterations. Iteration is an attempt to find equilibrium for that specific increment. The number of iteration depends on when equilibrium is reached see Figure 2.23 b). Sometimes the equilibrium condition cannot be fulfilled, the iteration diverge, ABAQUS analysis user´s manual 6.9 (2009).

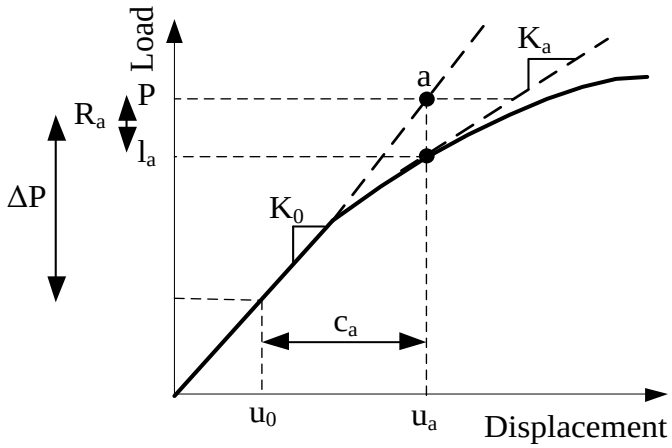

a)

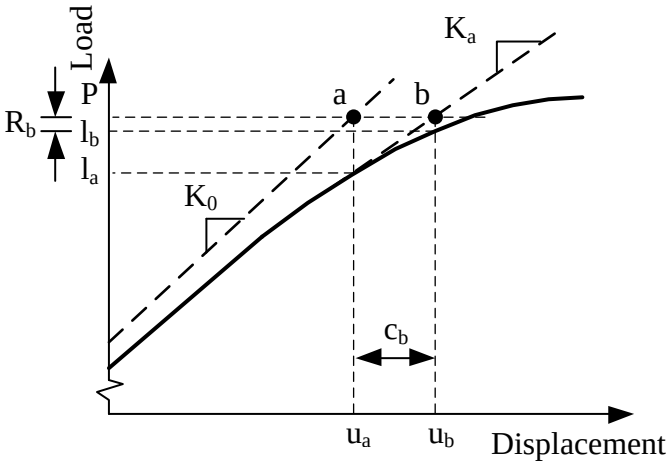

b)

Figure 2.23 a) The first iteration of a step, b) show the second iteration, based on ABAQUS analysis user´s manual 6.9 (2009).

2.5.5 Tolerance

For non-linear contact problems ABAQUS uses a relative tolerance for convergence. At each iteration, this tolerance is defined by default as $10^{\wedge -6}$ and this value is used in this thesis.

3 Experimental tests performed by SP Trätek

The following, briefly described, experimental tests performed by SP Trätek have been used as benchmark for the finite element models presented in Section 5 and in Section 6. The results from the experimental tests have also been used for verification of the results of the different models.

3.1 Full-scale test of a stress-laminated-timber deck

In December 2009, SP Trätek and Chalmers University of technology performed a full-scale test of two stress-laminated-timber decks in Skellefteå where the strength of the decks, when loaded up to failure load, was examined, Forsberg (2010). The test included two decks, with dimensions as shown in Table 3.1, where the first was a simply supported deck and the second one was a two span continuous deck. All beams were made of glulam made of spruce, with dimensions of 95 x 270 mm.

Table 3.1 Dimensions of the timber decks in the full scale test.

Deck	**Dimensions, *l* x *w* [m]**	**Number of beams**
Simply supported	5.4 x 7.98	84
Continuous	10.8 x 3.99	42

During the test, deformation measurements were performed for different levels of pre-stressing force and positions of the load. Pre-stress levels of 0.3 MPa, 0.6 MPa and 0.9 MPa were used and the load was placed in the middle and near the edge of the deck.

After the deformations was measured under various conditions the load was placed near the edge and with the pre-stress level set to 0.6 MPa the load was increased up to failure of the timber deck. The maximum load and deformation was registered.

To emulate a traffic load, similar to the main load model for road bridges used in Eurocode EN 1991-2, the load was applied to the timber deck by help of a distributing beam loaded with a hydraulic jack, see Figure 3.1. This beam applied a vertical load on two surfaces of 600 x 600 mm, with centre-to-centre distance of 2000 mm, at the same time, see Figure 3.2.

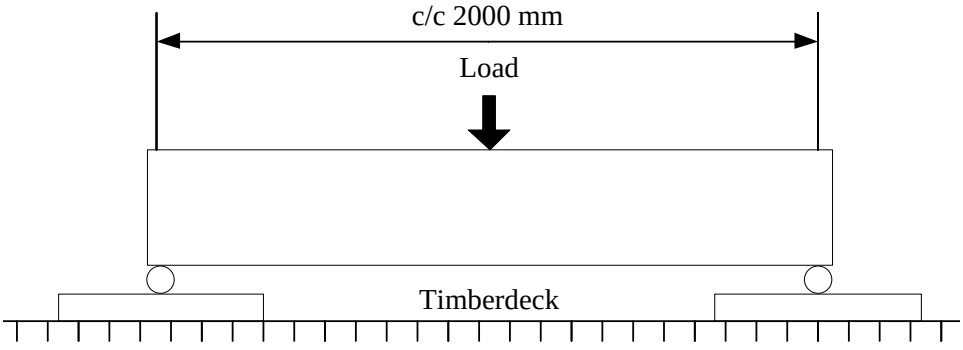

Figure 3.1 Distributing beam used to load the timber deck in the full-scale test.

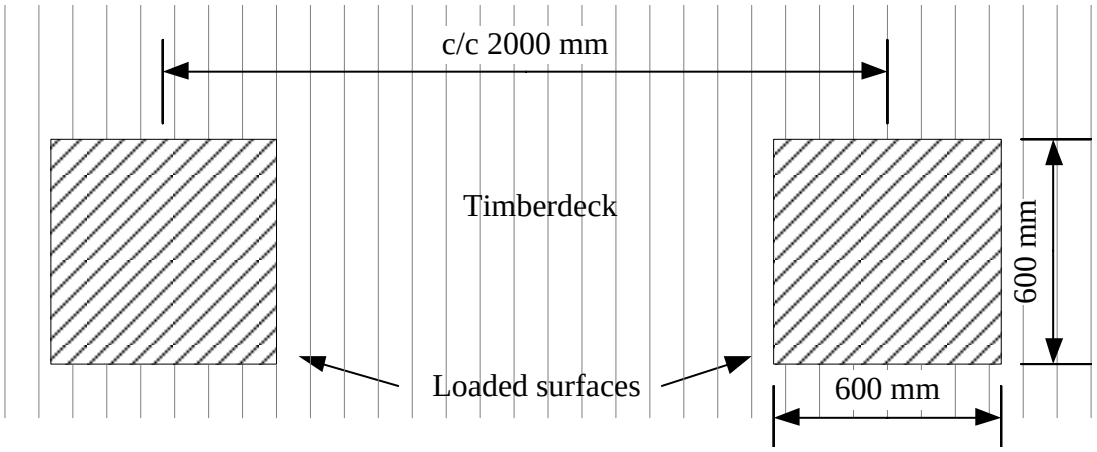

Figure 3.2 Loaded surfaces from the distributing beam.

The load application cycles used in the test is illustrated in Figure 3.3. For the deformation measurements, the loading was applied at a rate of approximately 200 kN/min in a sequence, up to the maximum value of 300 kN. At this load the deformations were measured in several points.

A similar cyclic load application, see Figure 3.3, was used when the load was increased up to failure at approximately 900 kN.

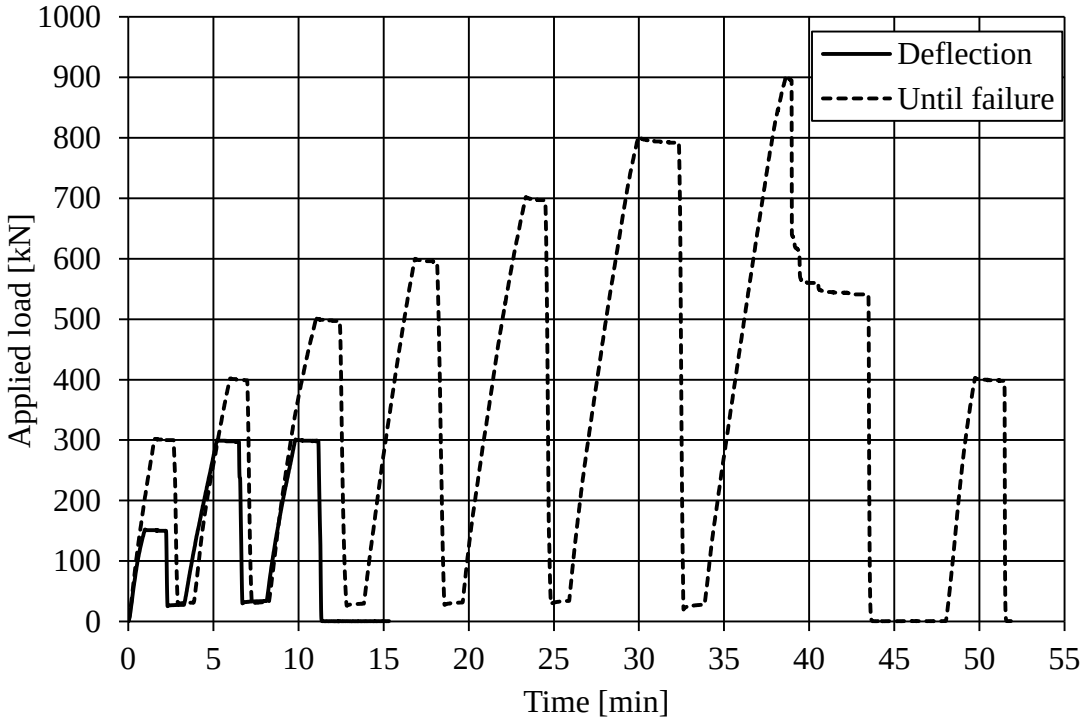

Figure 3.3 Load application cycle used in the full scale test performed by SP Trätek for two cases, measurements of deflection and loading until failure.

3.1.1 Results

The deflection was measured at different positions, i.e. sensors, transversal the stress-laminated deck at 300 kN. The largest deformations were measured directly under the loads whereas it evens out towards the unloaded edge. At the unloaded side the deflection is equal to zero due to the self-weight of the deck, which resist the deflection.

The deflection transversal the stress-laminated deck for three different levels of pre-stressing force under a load of 300 kN, placed at the edge of the timber deck, is showed in Figure 3.4. The deflection is larger for lower level of pre-stressing force. This type of curve will be used to verify the result from the finite element models.

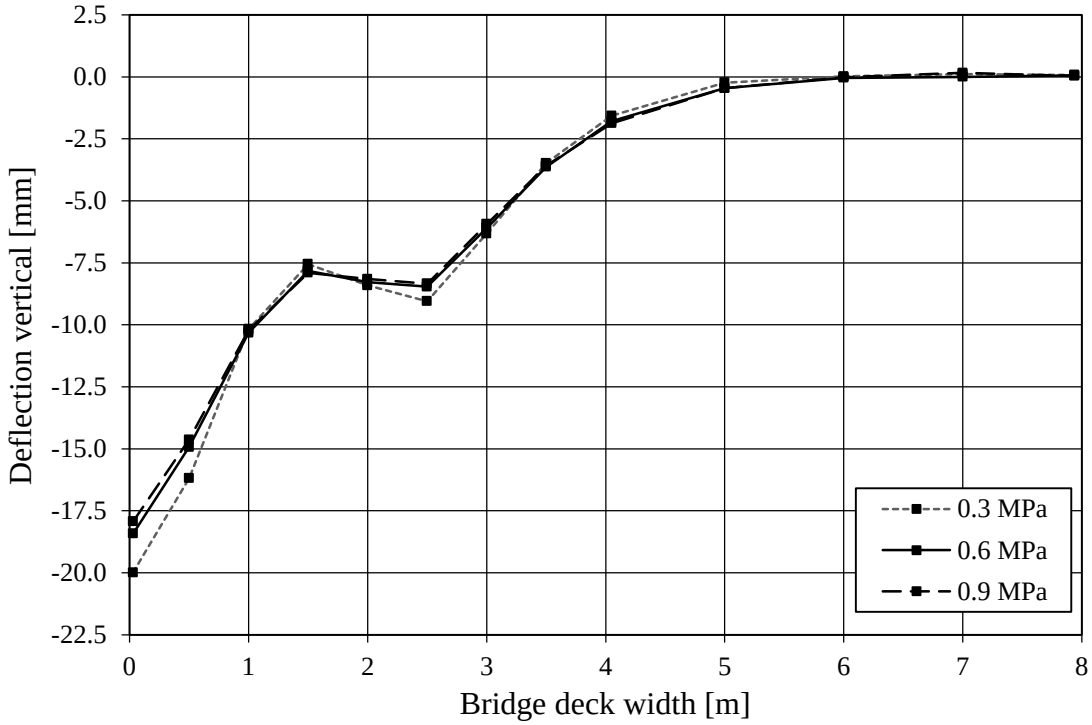

Figure 3.4 Deflection at 300 kN from SP full-scale test along bridge deck for different levels of pre-stress.

When the maximum load at failure was to be determined the stress-laminated-timber deck was pre-stressed at a level of 0.6 MPa and loaded with the edge load case. Maximum load before failure was determined to 900 kN with a maximum deflection at the loaded edge of approximately 65 mm.

The load deflection curve towards failure load, with a linear curve as reference, for the sensor placed at the loaded edge of the stress-laminated deck is showed in Figure 3.5. The response is clearly non-linear already from a small load, i.e. slipping and redistribution of the stresses in the deck occurs.

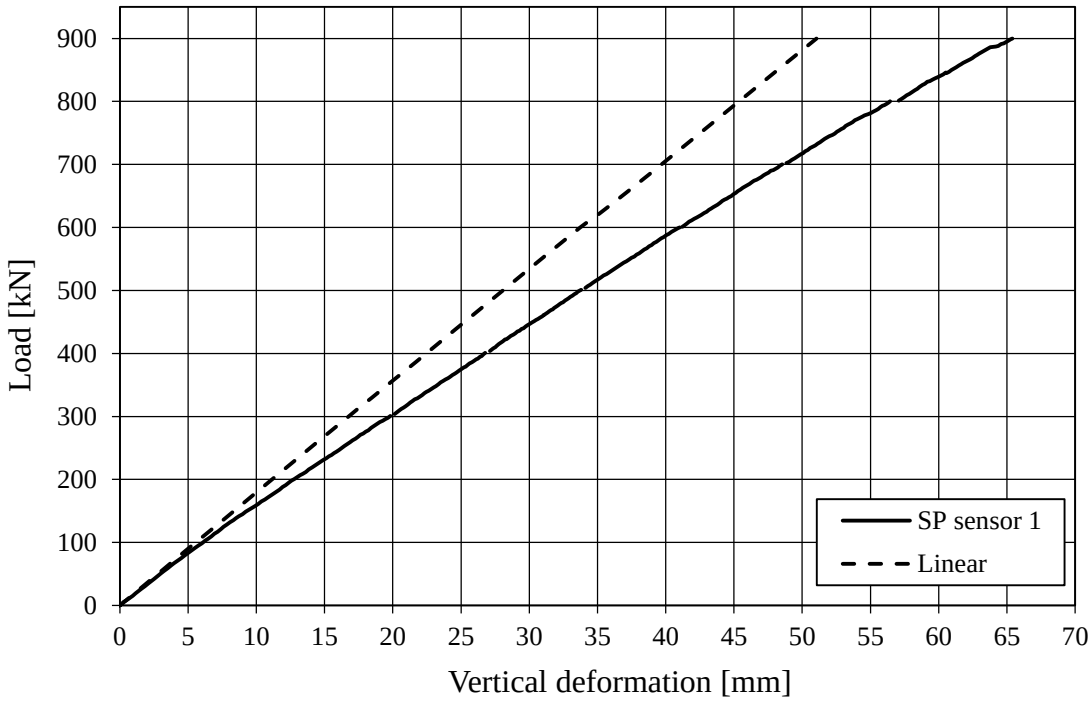

Figure 3.5 Load vs. deflection from SP Trätek full-scale test toward failure at 900 kN showing the non-linear response.

3.2 Frictional test

In September 2010, SP Trätek performed a frictional test in cooperation with Chalmers University of Technology, Forsberg (2010). The main purpose with this test was to obtain better knowledge about the frictional behaviour of timber at different levels of pre-stressing.

The test specimens were selected from the full-scale test described in Section 3.1. The shape of the specimens are showed in Figure 3.6 and were all planed spruce and had the dimensions of 180 x 180 x (38+78+38) mm.

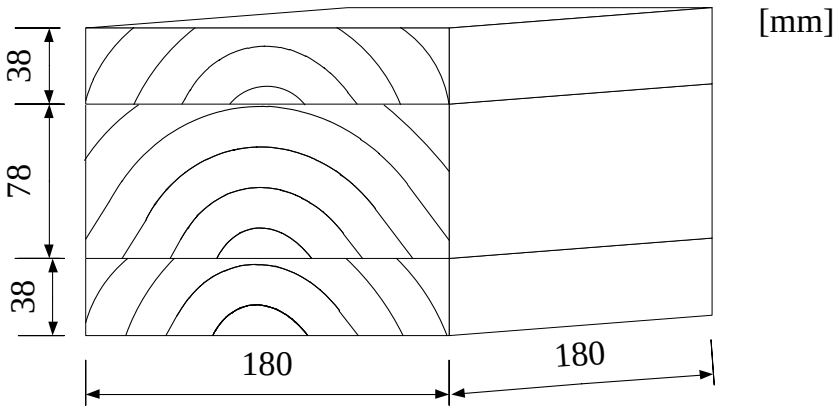

Figure 3.6 Shape and dimensions of test specimen in the frictional test performed by SP Trätek.

The specimens were all tested in a custom test rig, see Figure 3.7, and loaded with three different vertical loads, i.e. pre-stress levels of 0.3 MPa, 0.6 MPa and 0.9 MPa. The horizontal load was applied 90 degrees towards the vertical load. During the test the applied horizontal load and the displacements were registered, hence a frictional curve was achieved. In order to observe any differences, depending on fibre direction, the specimens were tested both in the parallel- and the perpendicular fibre direction.

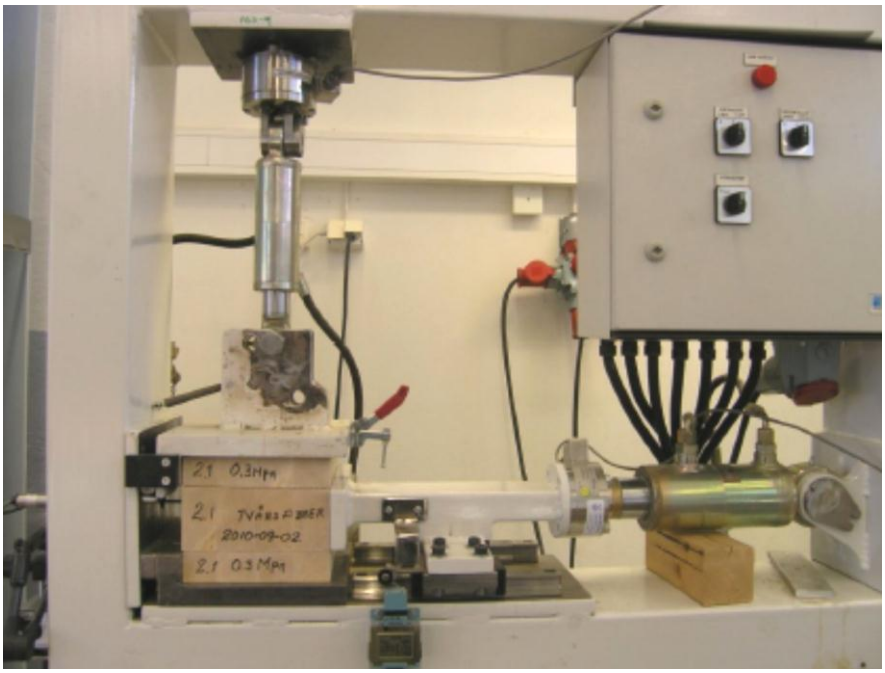

Figure 3.7 Test rig used in the frictional test, SP Trätek (2010).

The test included 48 tests with different specimens where the most of the tests were performed with a pre-stress level of 0.6 MPa. The reason for this was to be able to compare the result to the one from the full scale test were a bridge deck was loaded until failure. For the same reasons, the upcoming analyses and verifications in this thesis will mostly be performed at a pre-stress level 0.6 MPa.

3.2.1 Results

The large amount of tests produced a lot of different result curves. Because of large deviations in timber, the test results tend to have a relative large scatter. However, with large amount of data from experimental results certain trends can still be noticed and representative values can be picked out. To be able to compare the results, with a finite element analysis, modelled with a rather simple material model, these representative values have to be used in the comparison.

Some representative curves from the tests, when loaded parallel and transverse the fibres under a pre-stress level of 0.6 MPa, are showed in Figure 3.8 and Figure 3.9. The general behaviour of the response curves has similar shapes. The curves show a linear part in the beginning, with just a small deformation, when the load increases up to the maximum value. At this maximum load level the displacements increases suddenly with constant or decreased load level. This change can be explained by a

slip, i.e. the specimens start to move in relation to each other as the static friction is reached. When a slip occurs, the frictional properties changes from a static friction into a kinetic friction as described in Section 2.4.

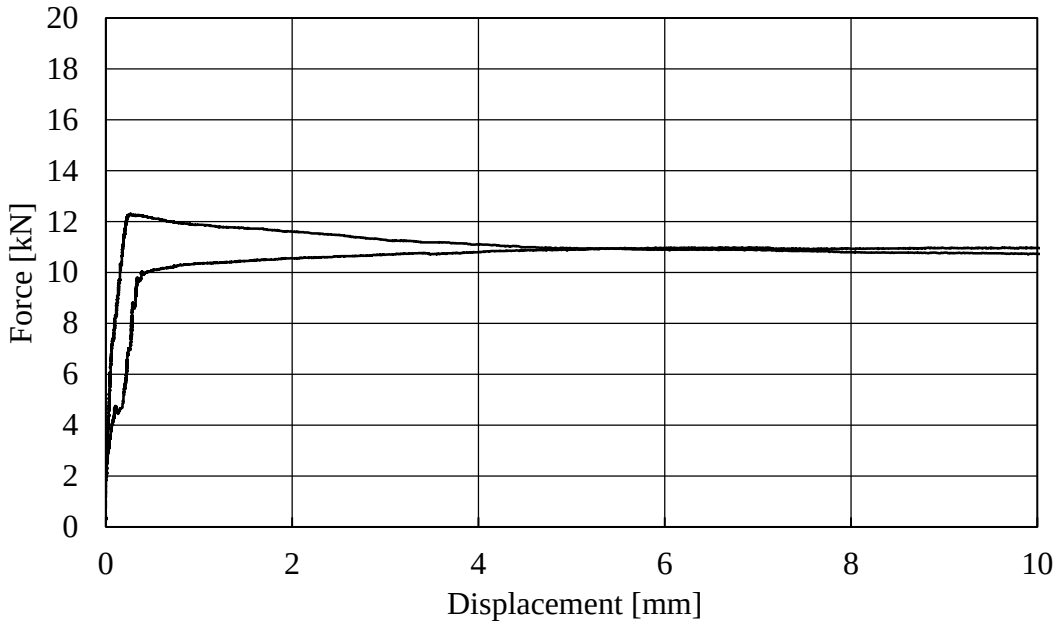

Figure 3.8 *Typical force-displacement result for load applied parallel to the fibre direction during test under a pre-stress level of 0.6 MPa, SP Trätek (2010).*

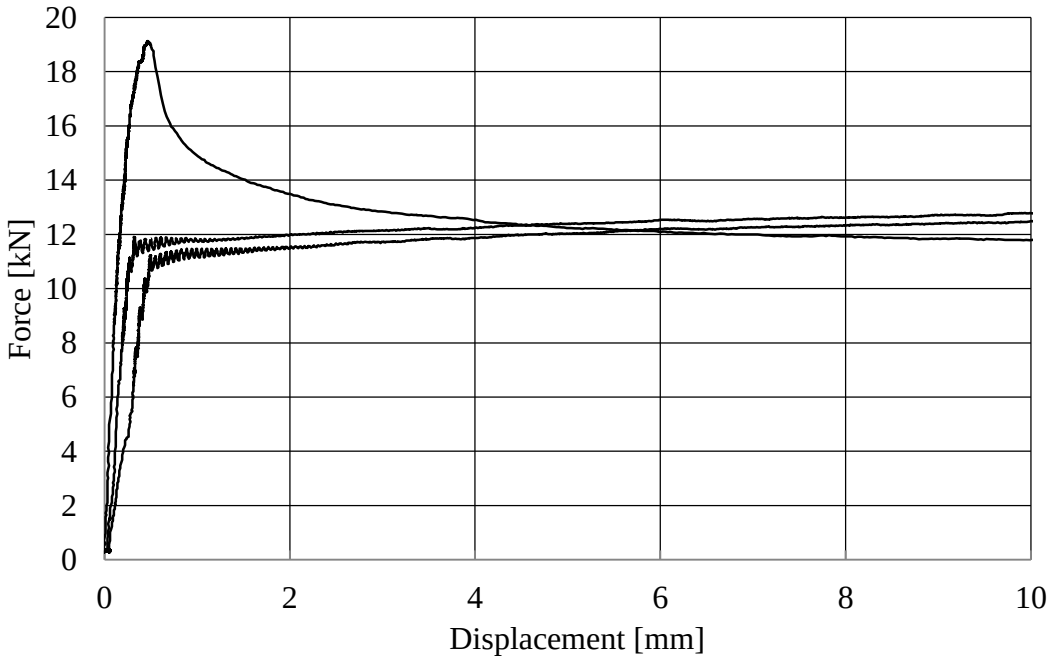

Figure 3.9 *Typical force-displacement result for load applied perpendicular to the fibre direction during test under a pre-stress level of 0.6 MPa, SP Trätek (2010).*

The magnitude of the maximum load differs depending on what fibre direction the test specimen is loaded in. The tests in which the load is applied perpendicular to the fibre direction a higher load is obtained prior to the development of the slip. Hence the friction coefficient is higher in the direction perpendicular to the fibres compared to the parallel direction. This also confirms the statement in Section 2.3.2 regarding friction coefficients.

3.2.2 Evaluation of the results

One of the most important results from the test is the maximum force. The behaviour after the maximum force is reached, i.e. when slipping occur, is more difficult to model and explain. In Section 5.3.1 the result will be compared to a finite element analysis and as a first comparison, the maximum force and the inclination of the linear part, i.e. the stiffness, will be verified.

The inclination of the curve up to the maximum force, i.e. the elastic slip or the stiffness, varies relatively much between the different specimens. In the following comparisons the same representative curve result will be used as in Section 3.2.1. However, just the first millimetre of movement will be studied. The curves shall be considered as extreme values and show a span of the values.

The results from loading applied parallel the fibres are showed in Figure 3.10. The slip points are indicated in the figure with a circle, and from this the elastic slip tends to vary between approximately 0.25 mm and 0.40 mm.

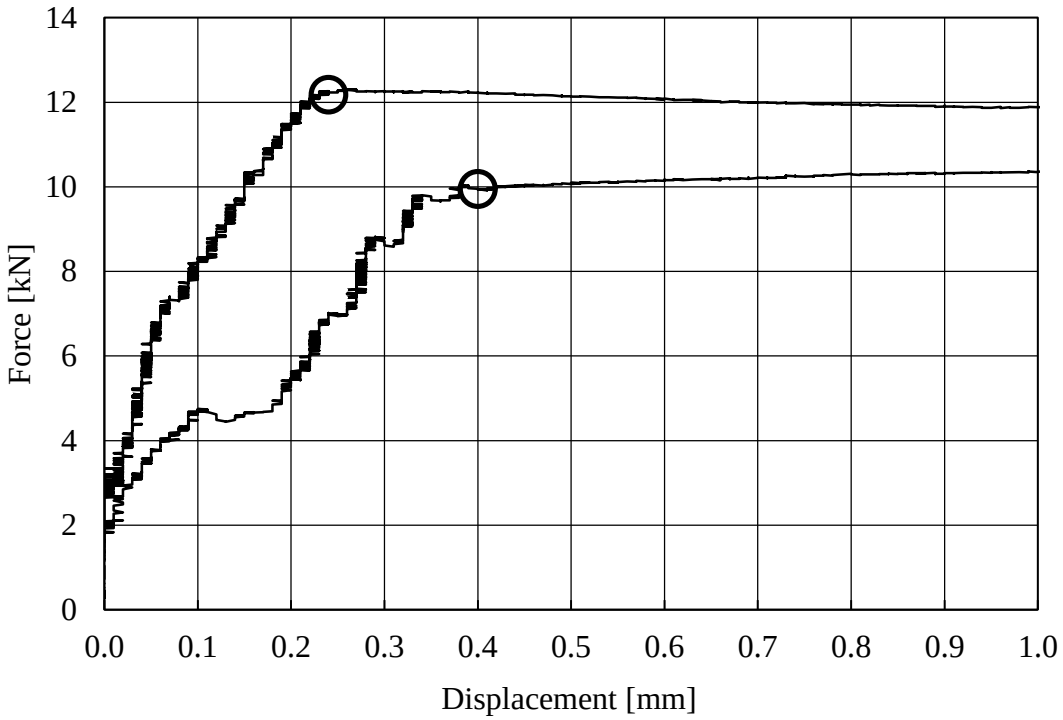

Figure 3.10 Study of the variations of the elastic slip, for load applied parallel to the fibre direction under a pre-stress level of 0.6 MPa. Two different extreme values for slip points are indicated in the figure.

Figure 3.11 shows the comparison, when loaded perpendicular the fibres, for three representative curves where two of them reach almost a similar maximum force while the other obtains a significantly higher maximum force prior to slip. For the two similar curves the slip point is indicated, with a circle, and the elastic slip tends to vary approximately between 0.30 mm and 0.50 mm.

For the result, which reached a significantly higher maximum force prior the slip point, the slip point is marked with a cross and it occurs approximately at 0.45 mm. It is interesting to notice the shape of the curve towards maximum force which is more curved than the others, i.e. the elastic deformations seem not to be linear for this case, or the deformations have an another behaviour.

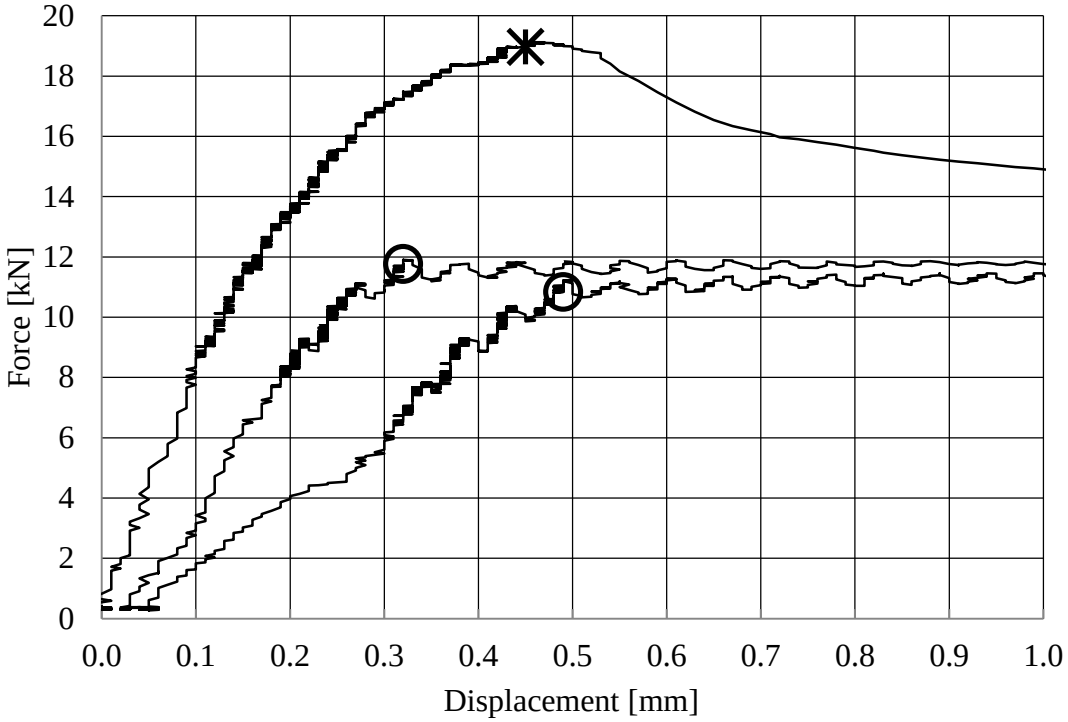

Figure 3.11 *Study of the variations of the elastic slip, for load applied transverse the fibre direction under a pre-stress level of 0.6 MPa. Three different extreme values for slip point are indicated in the figure.*

In general the spread in the results is larger when load is applied perpendicular the fibre direction than when loaded parallel the fibre direction. This concerns especially the maximum force obtained force prior to slip. This can be interpreted as the variations in frictional coefficient, μ, tends to be larger when loading perpendicular the fibre direction.

4 Model 1 – Box on a plane

4.1 Description

The first numerical model consists of a box placed on a plane, see Figure 4.1. The purpose of this simple model is to obtain better knowledge about how to model the frictional behaviour between solid elements in ABAQUS and be confident with the results obtained.

This model can be seen as a small part in a much bigger construction of several glulam beams put together side by side and forming a stress-laminated-timber deck. In this deck the beams are subjected to a certain load and during this an interlaminar slip can occur. This slip between two beams can by, applying several simplifications, be modelled as a moving box on a plane.

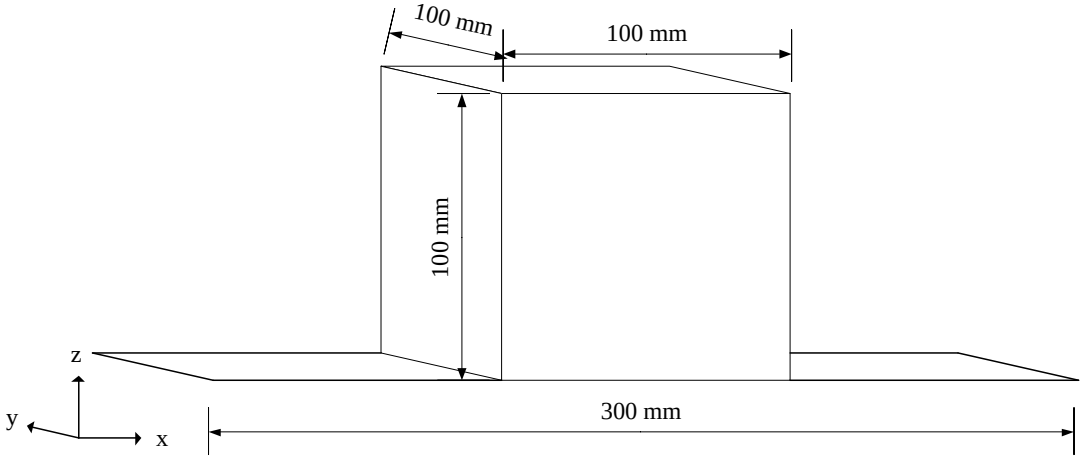

Figure 4.1 Model 1, box on a plane with actual dimensions.

4.1.1 Material properties

The box and the plane were established with 3D solid elements defined as deformable homogeneous materials. The box was assigned material properties roughly equal to the one for glulam while the plane was given stiff material parameters to be similar to a rigid plane, see Table 4.1. To simplify the interpretation of the results, a frictional coefficient, μ, of 0.5 is mostly used in the following analyses and the material behaviour is assumed to be isotropic.

Table 4.1 Material properties of model 1.

	Young's Modulus, E [MPa]	**Frictional coefficient, μ [-]**
Box	12 000	0.5
Plane	12 000 000	0.5

4.1.2 Prescribed conditions

The plane is assumed to be rigid and hence it is restricted to move and deform in any direction, therefore all degrees of freedom in the nodes on the plane are locked. The box is allowed to move along the plane but is restricted to move in the transverse direction to the plane, hence the translation in y-direction is locked.

The box is subjected to a vertical load of 1 kN. In ABAQUS the load is entered as a pressure load which for the given dimensions gives 100 kPa on top of the box. In the horizontal direction, a deformation controlled load is applied to the box as a prescribed horizontal displacement of 1 mm.

4.1.3 Element type

The model is defined with linear 8-node brick solid elements with reduced integration. Tests with quadratic 20 node elements, which in general is far better for bending problems, have also been made. However, this type of element is not possible to use for analyses involving contact between different parts, as for instance frictional behaviour, due to the miss balance in contact forces described in Section 2.5.1.

4.1.4 Mesh

The element size was chosen to 100 x 100 mm as a start value for the box and the plane which resulted in one element for the box and three for the plane. Tests of the effect with smaller mesh sizes were performed during the work.

4.1.5 Interaction

To define the interaction properties a contact pair was defined between the box and the plane consisting of the surfaces between the parts. For this model the first assumption was to use the penalty friction formulation together with isotropic material properties and an elastic slip of 0.5 mm. This means that the box is allowed to slip 0.5 mm elastically before it slide away, i.e. before the frictional force caused by the normal force and the friction coefficient is exceeded.

4.2 Evaluation

The predicted response for this model, when it is subjected to a vertical load and a horizontal displacement, is a frictional force which acts in the connecting surfaces between the box and the plane. This frictional force will have the form described in Section 2.4 and it is supposed to depend on the magnitude of the applied normal force and the size of the frictional coefficient.

To be able to check if the response of the model correspond to the theory about friction certain tests were made. To verify the basic law of friction various test was performed with a frictional coefficient of 0.5, defined with the penalty friction formulation. The other parameters as boundary conditions, load and mesh size was set as previously described. The values of the frictional forces in the following tests were mostly taken out from the nodes, connecting the surfaces, and summed up to represent the actual total frictional force.

4.2.1 Frictional behaviour

The frictional behaviour depends on the frictional properties of the actual surfaces in contact and the magnitude of the acting normal force. The expected result when running the analysis with different friction coefficients is higher frictional force for a higher coefficient of friction. As seen in Figure 4.2 the result for different coefficient of friction is corresponding to the basic theory about friction presented in Section 2.4.2. In this test the normal force, *N*, is set to 1.0 kN and the elastic slip is 0.5 mm.

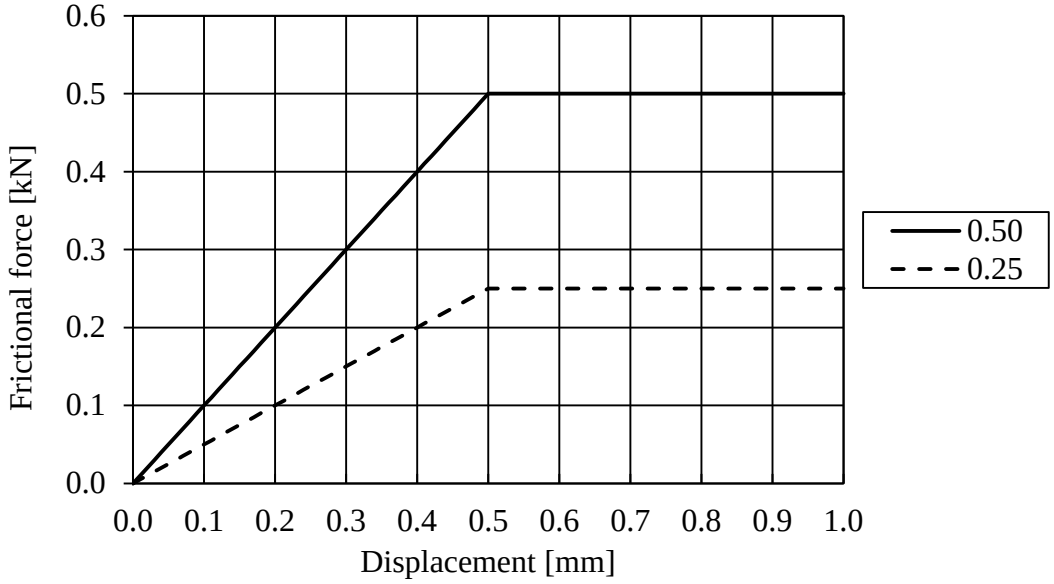

Figure 4.2 The effect on the frictional force from different coefficient of friction, μ.

The behaviour is also expected to depend on the size of the acting normal force. The frictional force is supposed to be higher when the normal force is higher. As seen in Figure 4.3 this is also the result in the analysis for two different magnitudes of normal forces. The response when the normal force is doubled is doubled frictional force. In this test the frictional coefficient, μ, is set to 0.5 and the elastic slip is set to 0.5 mm.

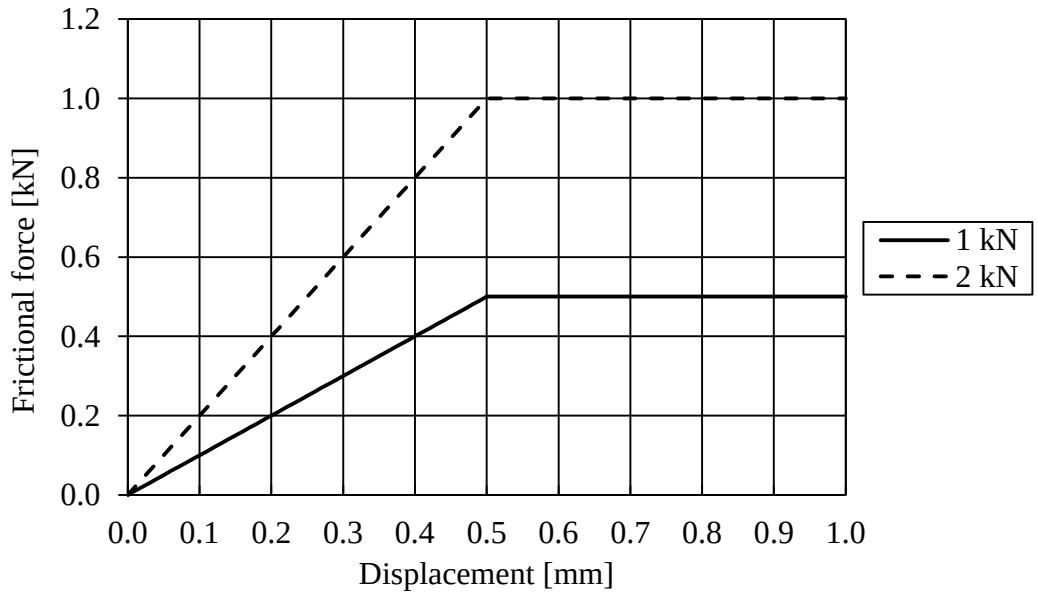

Figure 4.3 The effect on the frictional force from different level of normal force, N.

As a conclusion for these first tests one can say that the model seems to work, hence the interaction involving the frictional properties between the different parts seems to work properly.

4.2.2 Elastic slip

When certain frictional behaviour is to be assigned to the model, with help of the penalty friction formulation, the setting for the elastic slip distance is important. When choosing a small value the slipping phase should be reached earlier than when using a larger value. This difference in elastic slip distance can also be seen as a change in stiffness. The response for different elastic slip distances can be seen in Figure 4.4 where two different values of slip distance are tested to illustrate the behaviour. In this test the normal force, N, is set to 1.0 kN and the frictional coefficient, μ, is set to 0.5 mm.

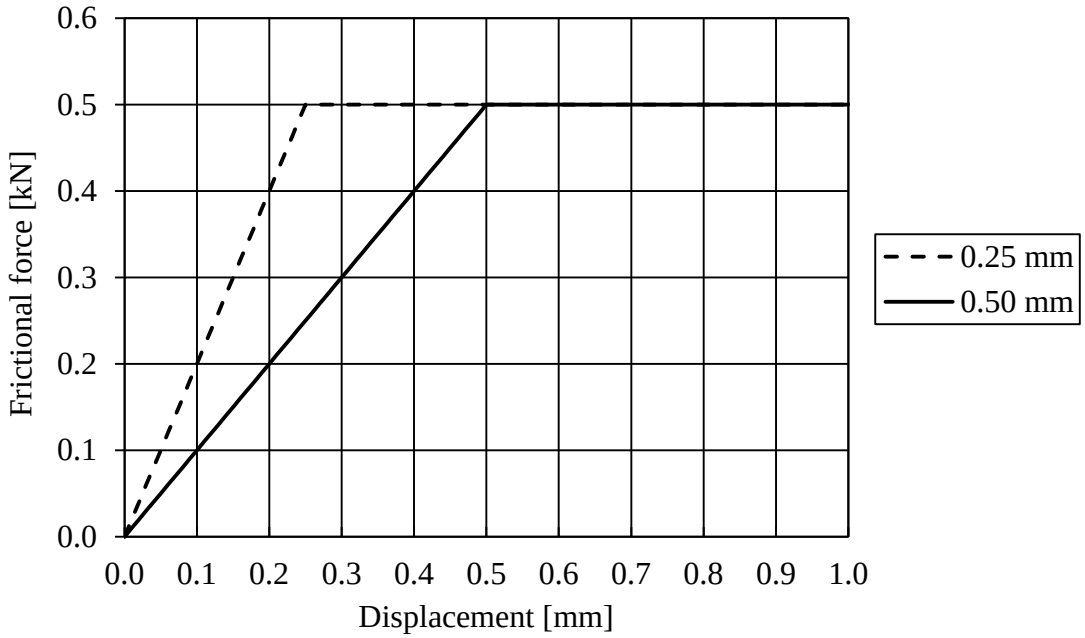

Figure 4.4 The effect on the frictional force due to different distance of elastic slip.

4.2.3 Time step

The size of the time step is important to obtain a correct solution. If the used time step is too large, the real solution may be hard to catch properly. Some points of interest, or even the real solution, can be missed. If, on the other hand, the time step is too small the computational time may be very long, whereas the result will not improve. In Figure 4.5 the curve appearance is showed for different number of time steps where the normal force, N, is set to 1.0 kN, the frictional coefficient, μ, is to 0.5 and the elastic slip is set to 0.5 mm.

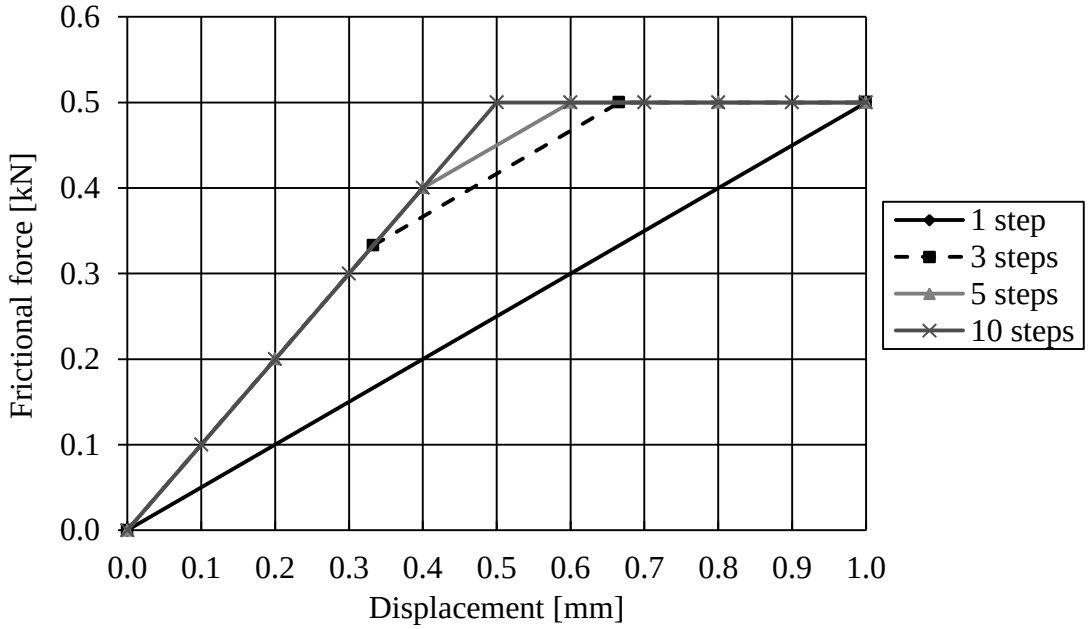

Figure 4.5 The effect on the frictional force for different number of time steps.

4.2.4 Load application

The deformation controlled load can be introduced in the model in different ways, e.g. it can be set to either move one surface or move a set of nodes. The most convenient is to apply the load as a displacement on both the edge surfaces of the box, hence move the front and back surfaces of the box, see Figure 4.6a. It is also possible to set the displacement at the specific nodes at the bottom sides of the box, see Figure 4.6b.

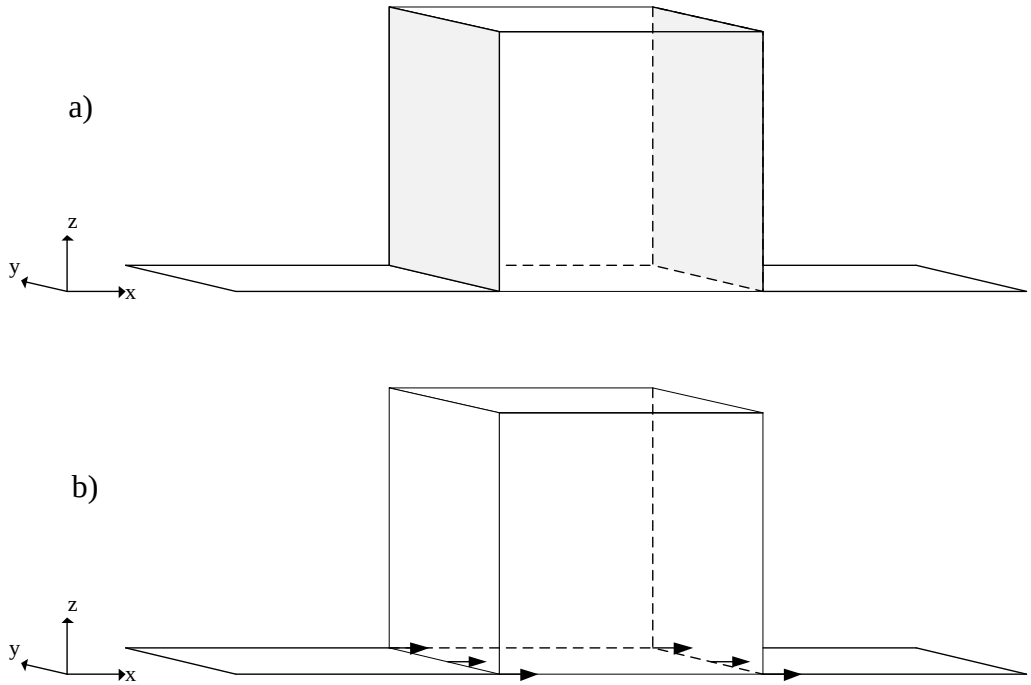

Figure 4.6 a) Displacement set at the surfaces of the box. b) Displacement set at the bottom edges of the box.

The results for the two different methods of load application are different. The expected result for resulting frictional force when moving the box over the plane is a constant frictional force as described in Equation 2.1. However, as illustrated in Figure 4.7, the frictional force differs along the side of the box. The frictional force is higher in direction of movement while it is lower in opposite direction.

When adding the displacement at the bottom nodes some numerical singularity problems at the boundary occurs which can be seen as the curves decreasing or increasing a lot at the ends. This behaviour is also spread into the nodes close to the boundary, which get a spiky response.

When applying the displacement at the surfaces of the box, as illustrated in Figure 4.6a, the behaviour is smoother and thus the effect of numerical singularities is not spread into the box in the same manner. The effect of the singularity, i.e. the magnitude of the stresses increases a lot in certain points, is also larger at the side opposite to the direction of movement.

In Figure 4.7 the difference in response is also shown for two different mesh sizes, which also is a factor that influences the behaviour. The mesh size affects the appearance of the curves in local points especially at points close to the edges of the box, but in a global view the curves can be approximated to follow the same path.

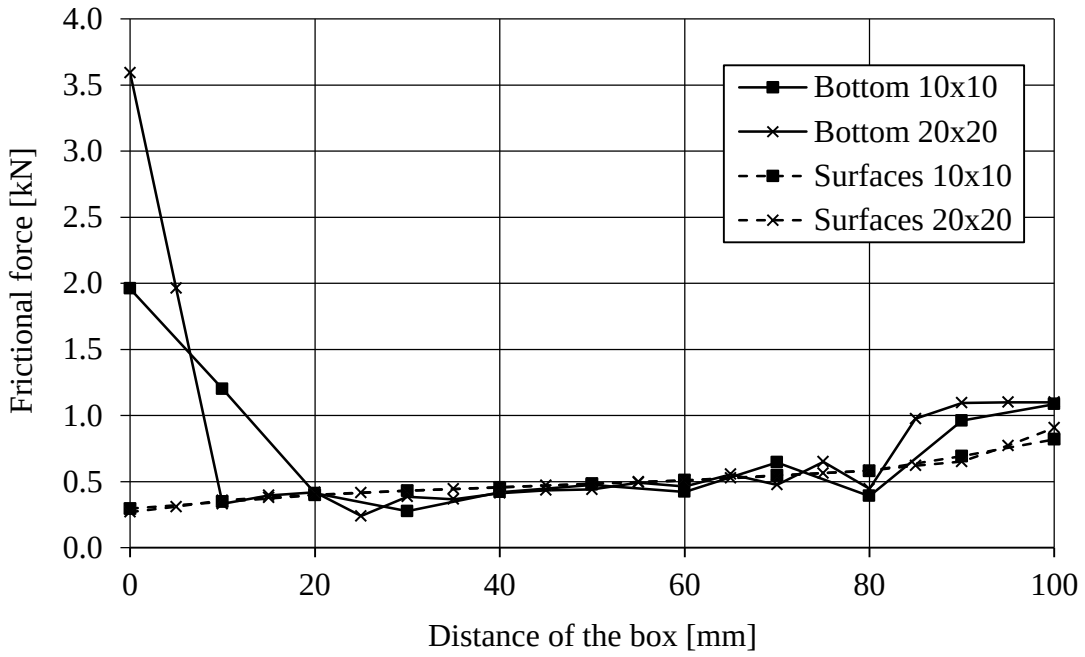

Figure 4.7 Comparison between the responses from different load application methods, as illustrated in Figure 4.6, for two different mesh sizes.

4.3 Results

When the box is moved over the stiff plane frictional forces appears between the parts. Referring to the direction which the box is moved in, the frictional forces, as illustrated in Figure 4.7, are larger at the front edge of the box than in the back side. This can be explained by that the frictional force acts as a retarding force on the box while it is moved along the plane.

In Figure 4.8 the behaviour of the box is illustrated. Before the box is moved along the plane a normal force, i.e. the pre-stressing force is applied at the top of the box. While the box is starting to move, by an initiated horizontal force, a moment is introduced to the box. The box gets compressed and even pushed down into the plane. This effect makes the box to want to tilt forward and thereby the compression forces, i.e. reaction forces in the figure, between the box and plane increase. This gives an increasing friction in the described area of the box.

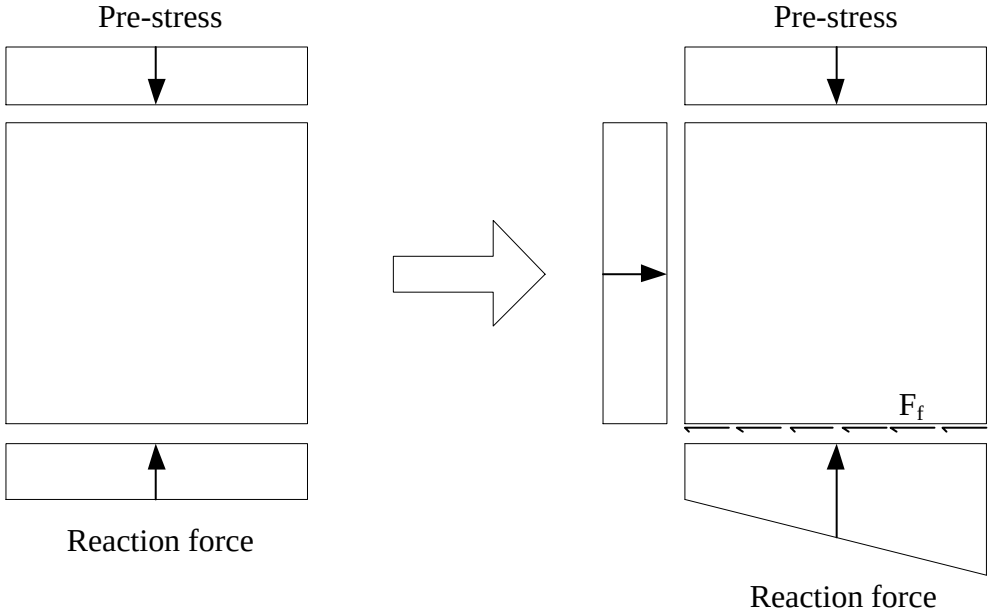

Figure 4.8 Retarding frictional force acting on the box when it is moving.

How to apply the displacement of the mode was determined to have influence on the result, especially on edges. When adding the displacement at separate nodes in the bottom of the box, numerical singularities was observed, which can be explained by the basis of the finite element method. When adding the displacement of the surfaces this behaviour was not observed

As a conclusion for model 1, the penalty friction formulation seems to be the most suitable for this type of analysis because it can model the frictional properties in a proper way and can be used for both isotropic and anisotropic material. When using the penalty friction formulation it is important to set a correct elastic slip distance. The elastic slip should be defined as an absolute value to be independent of the mesh size.

When defining the elastic slip distance it is also important to use an appropriate size of the mesh to get the expected result. To avoid obtain a faulty determined slip point, it is also important to use a correct size of the time step.

To be able to use different coefficients of friction for static and kinetic behaviour attempts to use the static-kinetic formulation was performed. However, the result was not satisfying because the decay parameter was hard to determine and control. The static-kinetic formulation can only be used for isotropic material properties and since anisotropic material properties is to be used later in this project it is important to use a formulation which can be extended to anisotropic material already from the beginning.

The Lagrange formulation is not appropriate due to the fact that the stiffness in the model can be of interest and the material will not be ideally plastic, hence no attempts to use this friction formulation were made.

5 Model 2 – Frictional test by SP Trätek

5.1 Description

The second finite element model, see Figure 5.1, is based on the frictional test performed by SP Trätek, briefly described in Section 3.2. To reduce the computational time, the model is made by use of symmetry properties. The symmetry line is set in the middle timber piece, hence it reduce the number of sliding surfaces from two to one. By this reason only half of the test setup, used by SP Trätek, is included in the model.

When the top plate is moving relative to the bottom plate a frictional force is induced and this force is the main interest in this analysis. Since symmetry properties is used in the model it is important to notice that the result from the finite element analysis is corrected due to this when it is compared to the experimental results.

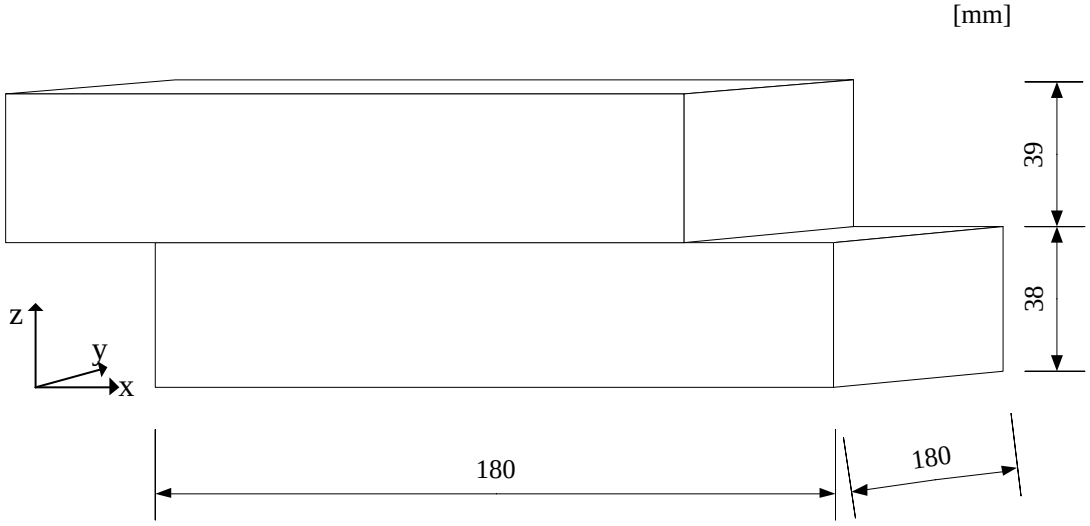

Figure 5.1 Model 2 based on the frictional test performed by SP Trätek.

5.1.1 Material properties

The two different timber plates were established as 3D solid elements defined as deformable homogeneous materials. Both of the plates are assigned material properties according to glue-laminated timber. The exact parameters of the test species, from the frictional test, are not well stated in the report from SP Trätek. By this reason the lower values, according to Persson (2000) showed in Table 2.1, was used as a standard case.

These material parameters are assumed at a moisture content of 12% and are reasonable starting values. However, the main focus of this model is to examine the response of different frictional behaviour. Hence the exact values of the other material parameters are not of great importance.

The coefficient of friction, μ, is different depending on the actual fibre direction of the timber plates. The frictional coefficient in the coming analyses is taken as mean values from the measured values in the SP Trätek frictional test. When loaded parallel

to the fibre direction the coefficient of friction, $\mu_{parallel}$ is 0.30 and when loaded perpendicular to the fibre direction the coefficient of friction, $\mu_{perpendicular}$ is 0.38.

The frictional behaviour is defined with the penalty friction formulation using isotropic frictional coefficient in the analyses. As the movement in this model is in one direction, isotropic properties of the frictional behaviour should be enough to use. However, it must be corrected by respect to the actual direction of movement for the timber plates.

5.1.2 Prescribed conditions

The model has boundary conditions as illustrated in Figure 5.2. At the left edge the lower plate is restricted to move in the x direction. The bottom plate has also a vertical support in the z direction.

A vertical load, *N*, representing the pre-stressing force is applied to the top plate. The horizontal load is applied as a prescribed deformation, *u*, at the right side of the top plate.

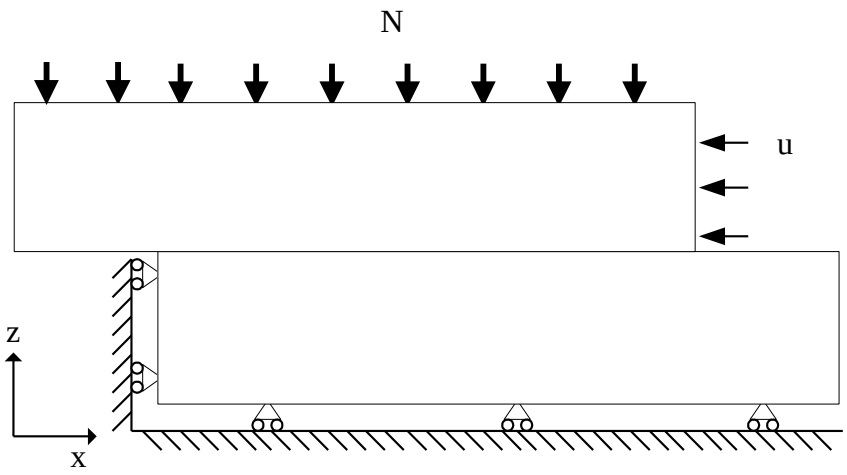

Figure 5.2 Model 2 with acting loads and boundary conditions.

5.2 Evaluation

5.2.1 Anisotropic friction

Use of anisotropic friction properties, i.e. different properties in different directions, is possible in finite element analysis in ABAQUS using the penalty friction formulation. However, when changing the frictional properties from isotropic to anisotropic no change in the behaviour was registered in this case. This was also the expected result as the movement was just in one direction, i.e. isotropic behaviour should be enough in the modelling of this problem.

5.2.2 Mesh size

The influence from different mesh sizes on the maximum force level is of interest. As shown in Figure 5.3 the maximum force reached, before the friction force is overcome by the applied force, is approximately 7.25 kN when using an element size of 180 mm

(1 x 1). However, when refining the mesh to 60 mm (3 x 3) the maximum force obtained is approximately 7.40 kN, i.e. the result changes. When refining the mesh size to 18 mm (10 x 10) just a small increase in difference can be noticed.

As shown in Figure 5.3 the first refinement of the mesh size also affects the shape of the curve up to the maximum level, i.e. the stiffness tends to be slightly higher. This observation is important and the mesh size has to be kept in mind as a factor when comparing to test results. After these analyses the appropriate mesh size for the timber plates was determined to 60 mm.

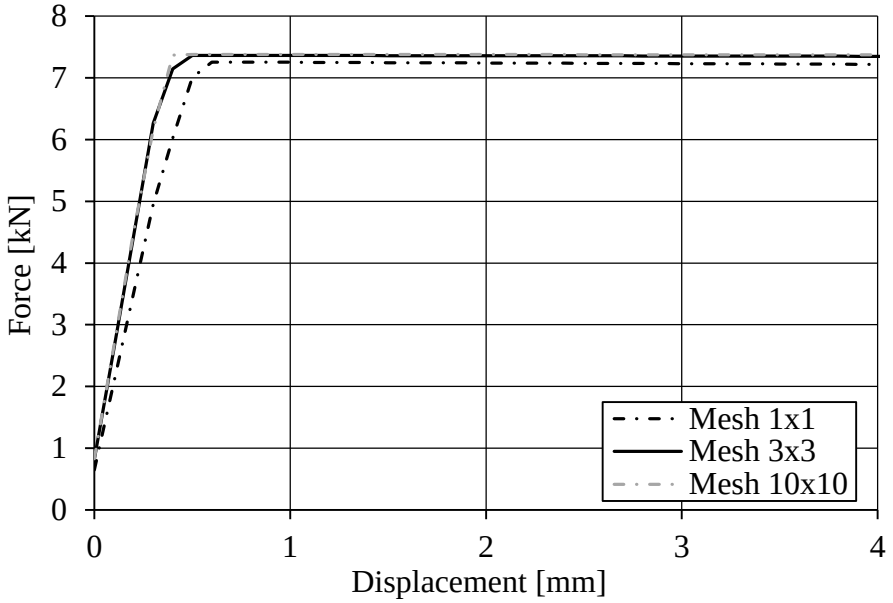

Figure 5.3 Different mesh sizes for model 2, loaded perpendicular to the fibre direction under a pre-stress level of 0.3 MPa.

5.2.3 Material properties

To investigate whether different material properties of the glulam plates have some effect on the result, a test with increased material properties was performed. The higher material properties were chosen as the higher values in Table 2.1 according to Persson (2000) and is overall approximately 25% higher than the case considered as the standard values. This test was performed under a pre-stress level of 0.3 MPa and a mesh size of 60 mm.

As shown in Figure 5.4, no difference in the response for different material parameters was observed. Hence, this test represents the true frictional response which, as described in Section 2.4.2 depends on the magnitude of the normal force and the coefficient of friction.

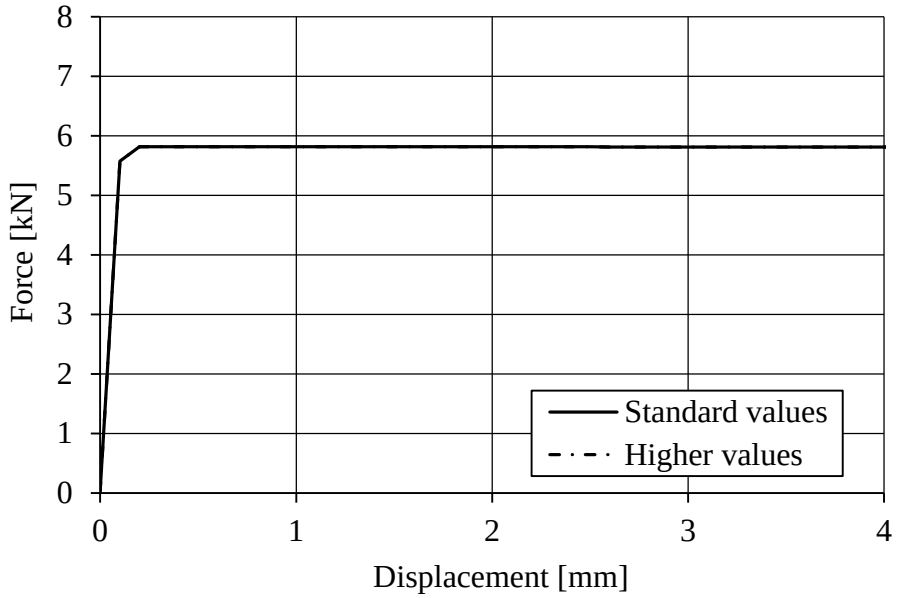

Figure 5.4 *Different material properties for model 2, loaded parallel to the fibre direction under a pre-stress level of 0.3 MPa, elastic slip 0.5 mm and μ=0.3.*

5.3 Results

5.3.1 Finite element model vs. experimental test by SP Trätek

It is not possible to model the real response after slipping in this type of analysis, i.e. when the maximum force goes down whereas the deformations increase. This type of analysis is good towards the maximum force prior the development of the slip. The comparison of maximum obtained force was performed for two different load cases: load applied parallel to the fibre direction and load applied perpendicular the fibre direction, whereas the pre-stress level was constant at 0.3 MPa.

The expected maximum force, before the friction force is overcome by the applied force, was the value obtained from the frictional test performed by SP Trätek, described in Section 3.2. As described in Section 3.2.1 there is a relative large scatter in the results from the SP Trätek frictional test. To compare and evaluate the result from the finite element analysis to the test results some representative curves was picked out from the tests.

As shown in Figure 5.5 the test results from SP Trätek show two different types of behaviour for the case of load applied parallel to the fibres of the timber. The result from test number two is similar to the numerial finite element result whereas the result from test three is not as similar to the numerical result. However, when comparing the maximum obtained force in the tests versus numerical analysis, the result is good. The maximum obtained force when the load is applied parallel to the fibre direction is approximately between 5.4 kN and 5.7 kN whereas the finite element result is 5.7 kN, hence a good correspondence.

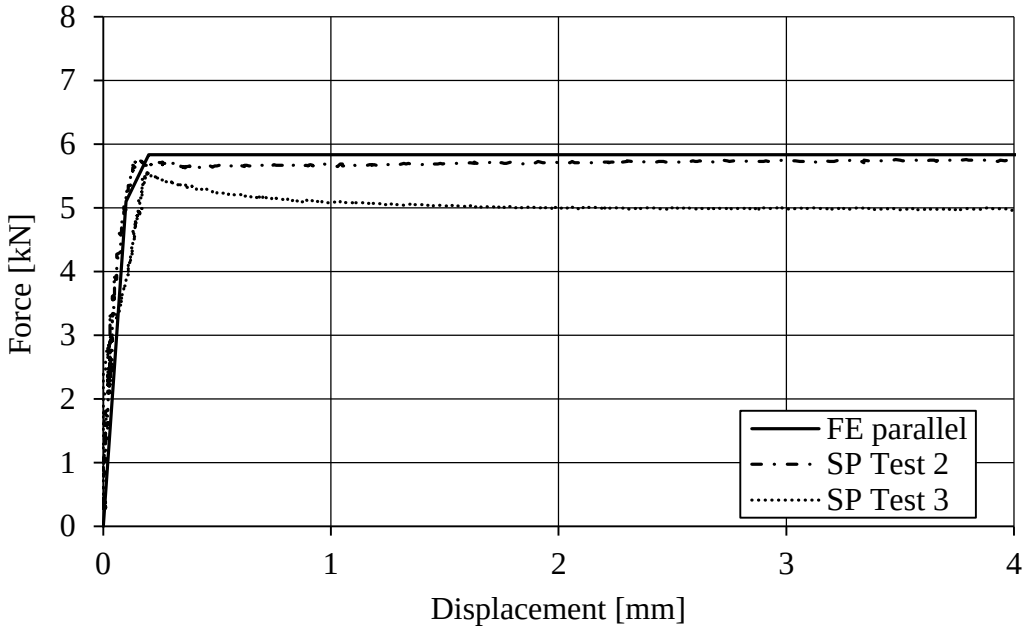

Figure 5.5 *Comparison between the result from the finite element model and SP Trätek test, loaded parallel to the fibre direction under a pre-stress level of 0.3MPa.*

The results, for the case load applied perpendicular to the fibre direction of the timber, are compared and in Figure 5.6. The maximum force is between approximately 6.9 kN and 10.4 kN for the SP Trätek tests. The numerical analysis produce the maximum force of approximately 7.3 kN, so when comparing to the experimental result, the analysis shows a lower value. However, the differences in test result, both in terms of obtained maximum force and slip point, are larger when the load is applied perpendicular to the fibres than for the case when the load is applied parallel to the fibres.

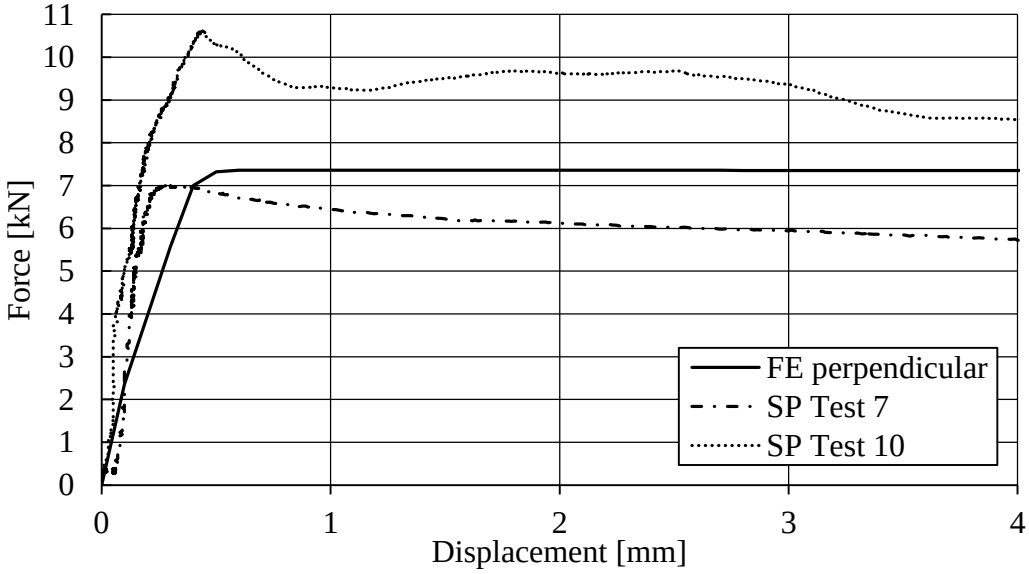

Figure 5.6 *Comparison between result from the finite element model and SP Trätek test, loaded perpendicular to the fibre direction under a pre-stress level of 0.3MPa.*

Since the finite element model analysis use mean values of the coefficient of friction, μ the maximum force sometimes is too low. More interesting is the response up to the maximum force, i.e. the elastic slip. In both Figure 5.5 and Figure 5.6 the response up to the maximum force, i.e. the elastic slip, is similar to the test result. To obtain these results, an elastic slip of 0.1 mm was used in the finite element analyses, i.e. a smaller value than the approximated interval in Section 3.2.2.

It is interesting to notice that, when applying the load perpendicular to the fibres and using an elastic slip of 0.1 mm, the slip point in Figure 5.6 is obtained at approximately 0.40 mm instead of the expected 0.10 mm. The low stiffness of glulam in the tangential direction, E_T, which is the actual direction of movement in this analysis, is a possible explanation of this difference. The deformation of the timber plate is larger than the elastic slip distance and hence the elastic slip becomes larger than expected. This behaviour was also discussed in Section 3.2.2 as a reason to the result from the frictional test performed by SP Trätek.

In Section 5.2.3 a test of changed material parameters was performed where no differences in the result was noticed, see Figure 5.4. However, that analysis was performed with movement parallel to the fibres, i.e. the longitudinal was decisive for the deformations. While the longitudinal stiffness is significantly higher than the tangential, no large deformation was observed, even for changed material parameters of 25%. It is concluded that to use low elastic slip, a sufficiently high stiffness is required. The deformations noticed in Figure 5.6 can be explained by a structural effect rather than a material dependent reason.

However, in general the result and response from the finite element analyses are good for model two. The results depend a lot on the coefficient of friction and the size of the elastic slip. The analyses performed are based on coefficients of friction which are estimated mean values from the SP Trätek tests. Probably those values are too inadequate when comparing this into such detail, but to determine those exactly is hard due to the large variations the material properties of timber.

6 Model 3 – Full-scale test by SP Trätek

This section presents the work with the finite element model consisting of an entire stress-laminated-timber deck that consists of a large number of glulam beams which are pre-stressed together. The deck was modelled as the simply-supported deck, with dimensions of 5.4 m x 7.98 m, in the full-scale test performed by SP Trätek presented in Section 3.1.

In the full-scale test the deck was loaded up to failure with the load placed at the edge of the deck, hence the finite element modelling will focus on the edge load case.

6.1 Model 3a - one beam

Before the entire deck, consisting of several beams, was modelled, one beam was picked out and analysed. This beam was used in the verification of the model which was conducted by comparing bending- and shear stresses and the deflection at mid span with the results from static hand calculations. By doing so it was possible to determine an appropriate mesh size to use in the larger 84 beams model.

The beam was treated as a simply-supported beam subjected to a uniformly distributed load of 10 kN/m, see Figure 6.1. Material parameters used were corresponding to mean values of the properties given in Table 2.1, Fortino and Torrati (2008).

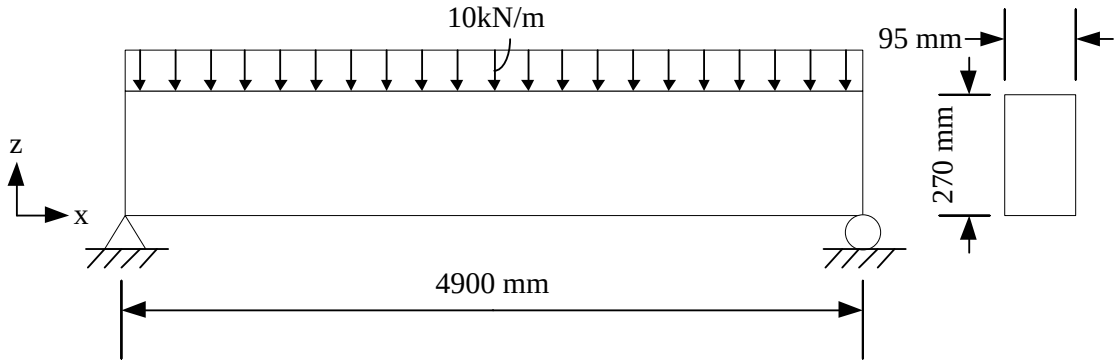

Figure 6.1 Illustration of the beam in model 3a with dimensions and acting load.

6.1.1 Mesh size with respect to bending stresses and deflection

To determine if the result from the finite element analysis was accurate it was compared to hand calculations, performed for maximum vertical deflection, u, and maximum bending stress, σ_x. The following analyses were made with different element types and mesh sizes in both height- and longitudinal direction. The mesh size for the beam was determined to give a result considered as good enough, which is a justification regarding to calculation time and the final result.

Maximum vertical deflection, u, in the middle of the beam was calculated according to Equation 6.1, where the first part is deflection due to flexural bending and the second part is deflection due to shear. The maximum bending stress in the x-direction, σ_x, was calculated according to Equation 6.2

$$u = \frac{5 \cdot q \cdot L^4}{384 \cdot E \cdot I} + \frac{1.2 \cdot q \cdot L^2}{8 \cdot A \cdot G} \quad (6.1)$$

E = Young's Modulus

G = G_{xz} = Shear modulus

$$\sigma_x = \frac{M}{W} \quad (6.2)$$

M = Maximum moment in mid span

W = Bending resistance of the cross-section.

In Table 6.1 and Table 6.2 the finite element result is showed for different combinations of mesh size and element type, compared to the hand calculated values. The analysis performed with 20 node elements was expected to give better results than the 8-node elements, especially for bending stresses. Further, a finer mesh should obtain a more accurate result than a coarse mesh compared to the results from hand calculations, but with cost of computational time.

From the analyses it was determined that a mesh size of 45 mm in height direction and 100 mm in longitudinal direction was good enough to represent a correct deflection and bending stress. It was also showed that the 20 node element gives a good result for a course mesh, however, to be able to use contact properties between several beams to model the frictional behaviour this element type is not applicable, see Section 2.5.1. From this 8-node solid elements was chosen.

The difference in vertical deflection between the hand calculation and finite element analysis can be explained by the fact that the hand calculation does not take the local deformation perpendicular to the fibres at the support into account. In the finite element analysis this is taken into account which explains the slight difference.

Table 6.1 Comparison between different mesh sizes in the longitudinal direction when mesh size in height direction is fixed to 45 mm.

Element type	**Mesh size x-direction**	**Bending stress σ_x-direction**		**Deflection z-direction**	
	[mm]	[MPa]	[%]	[mm]	[%]
Hand calculation	-	**5.3**	-	**8.6**	-
8-node solid, C3D8R	200	4.5	-14.2	9.0	4.4
8-node solid, C3D8R	100	4.5	-14.2	9.0	4.4
8-node solid, C3D8R	50	4.5	-14.2	9.0	4.4
20-node solid, C3D20R	100	5.3	0.8	8.7	1.1

Table 6.2 Comparison between different mesh sizes in height direction when mesh size in the longitudinal direction is fixed to 100 mm.

Element type	Mesh size z-direction	Bending stress σ_x-direction		Deflection z-direction	
	[mm]	[MPa]	[%]	[mm]	[%]
Hand calculation	-	**5.3**	-	**8.6**	-
8-node solid, C3D8R	135	3.5	-33.4	11.6	25.9
8-node solid, C3D8R	90	4.0	-24.9	9.8	12.2
8-node solid, C3D8R	67.5	4.2	-20.0	9.3	7.5
8-node solid, C3D8R	54	4.4	-16.6	9.1	5.5
8-node solid, C3D8R	45	4.5	-14.2	9.0	4.4
8-node solid, C3D8R	33.75	4.7	-10.8	8.9	3.4
8-node solid, C3D8R	27	4.7	-10.8	8.9	3.4
20-node solid, C3D20R	45	5.3	0.8	8.7	1.1

6.1.2 Mesh size with respect to shear stresses

To find the size of the mesh in the height direction of the beam that was necessary to represent the shear stresses in the beam properly the following analysis was performed. The desired shape of the shear stress curve, τ, is the parabolic shape provided from the analytical hand calculation of the shear stress. The analytical calculation was performed according to Equation 6.3.

$$\tau = \frac{S \cdot V}{I \cdot b} \tag{6.3}$$

S = First moment of area V = Shear force

I = Moment of inertia b = Width of the beam

The stress concentration close to the support acts as a disturbing factor when looking at the shear stresses close to the support of a beam. To determine at which distance the shear stresses can be considered as undisturbed, stresses at different distances from the support was compared, see Figure 6.2.

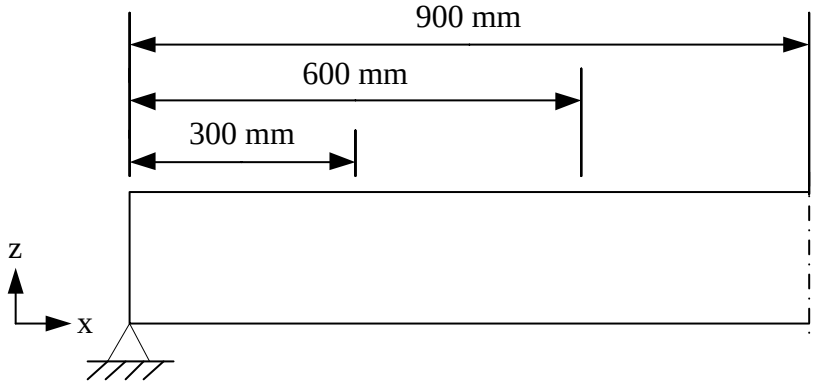

Figure 6.2 Illustration of where in the beam the different sections are taken.

The shear stresses from the numerical analyses, at different distances from the support, are compared to the analytical shear stress in Figure 6.3. At 300 mm from the support the stress was disturbed a lot, but when looking at a distance of 600 mm and 900 mm from the support the stress showed a shape that was more similar to the analytical shear stress curve. Hence it was concluded that the mesh comparison regarding the shear stresses has to be made at least 600 mm from the support.

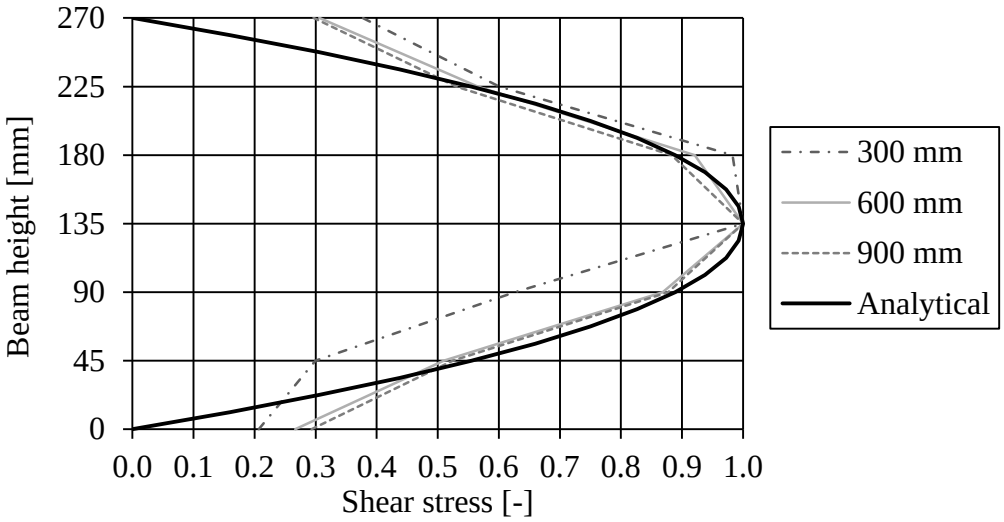

Figure 6.3 Shear stress, τ_{xz}, for mesh 45 mm at different distances.

The shear stresses, τ_{xz}, at 600 mm from the support are shown for different mesh sizes in Figure 6.4. As showed a mesh size of 45 mm gave a fairly good result but when reducing the mesh to 22.5 mm the shape of the obtained curve was smoother and more similar to the analytical curve. The difference between 22.5 mm and 11.25 mm was very small and hence 22.5 mm should be good to use.

However, to reduce computational time it was here concluded that using a 45 mm mesh was still sufficient to produce results considered as good enough, since the main purpose in this thesis was not to investigate the shear stresses in detail.

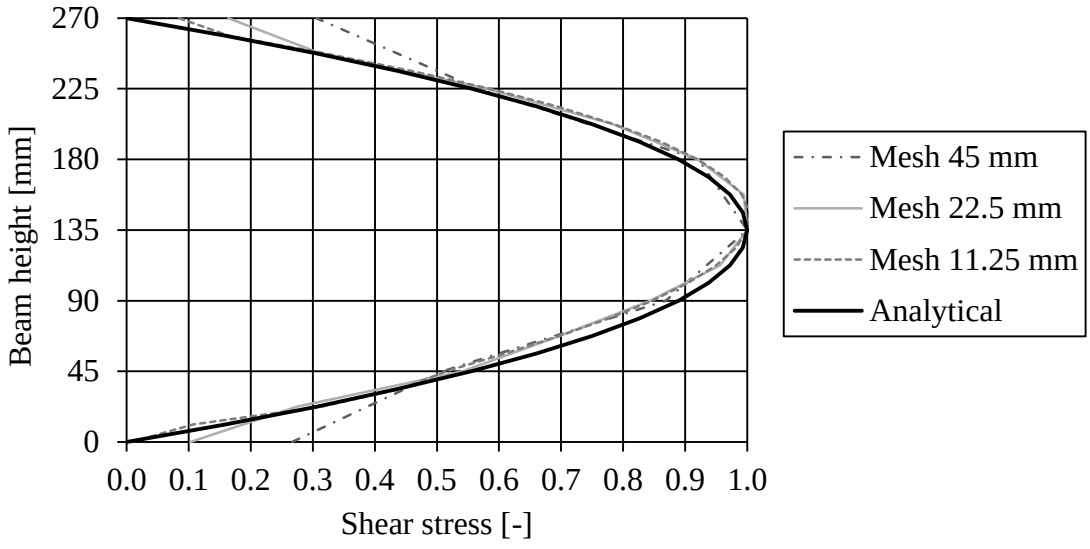

Figure 6.4 Shear stress, τ_{xz}, for different mesh sizes at 600 mm from the support.

6.2 Model 3b – 84 beams stress-laminated-timber deck

6.2.1 Geometry

In Figure 6.5 the dimensions and load placement of model 3b is illustrated. This model consists of 84 beams, similar to the beam in model 3a, put together as a stress-laminated-timber deck. The beams in the full-scale test had dimensions of 270 x 95 x 5400 mm and the deck had a total width of 84 x 95 mm, i.e. 7980 mm. To reduce the computational time, symmetry boundary conditions were used in this numerical finite element model, thus only half the deck is modelled. Hence the actual length of the beams in the coming analyses was 2700 mm.

In the full-scale test the deck was simply supported on two steel beams of width 100 mm. In the analysis it was modelled as simply supported on the steel beams with a frictional coefficient, μ=0.5 between steel and timber.

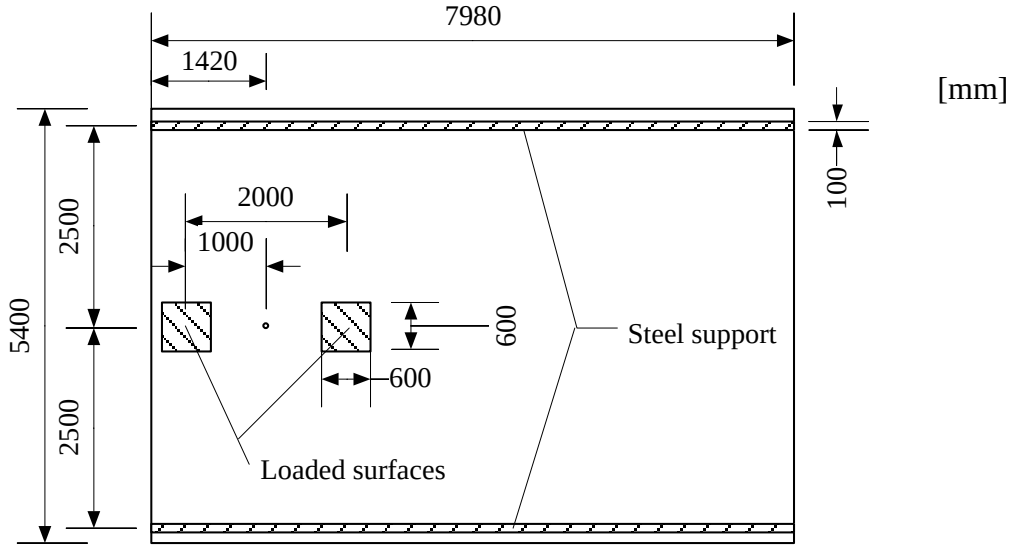

Figure 6.5 Model 3b, dimensions and placement of the load.

6.2.2 Load application

The self-weight of the timber deck was considered to 500 kg/m^3 which were added as a gravity load to the model. To restrain the uplifting at the supports when the deck is loaded it is important to include the self-weight. However, when comparing to the test-results it must be removed from the result for it to be accurate.

The deck had a pre-stressing force applied at the ends as uniformly distributed pressure loads, hence a simplification to the real pre-stressing rods used in the full-scale test. This pre-stressing force was mostly set to 0.6 MPa in the analyses to be able to verify the result to the SP Trätek failure test.

The actual load on the deck, from the distributing beam described in Section 3.1, was applied to the model as surface pressure loads at two surfaces indicated in Figure 6.5. The self-weight of the distributing beam was also added as an extra load to the surfaces. The distributing beam was placed with its centre at 1420 mm from the bridge deck edge. Use of symmetry boundary condition in the length direction gave the actual loaded surface in the model to 0.3 m x 0.6 m, i.e. the symmetry line is going

through the loaded surfaces. The loading from the distributing beam was applied as pressure loads of 5555.5 Pa/kN which corresponds to the actual size of the surfaces.

6.2.3 Material properties

From the earlier models in this thesis some initial material data and other model settings was given, and hence it defined the case called "standard case", see Table 6.3. From this standard case several test and modification was performed which also may change the case considered as standard case. The material properties used for the standard case is mean values according to Fortino and Torrati (2008), shown in Table 2.1. Friction formulation used was the penalty formulation with anisotropic frictional behaviour and frictional coefficient as mean values from SP Trätek frictional test.

Table 6.3 Material properties for model 3c, also called standard case.

Young's modulus	**E_L [MPa]**	**E_T [MPa]**	**E_R [MPa]**
	12000	600	600
Shear modulus	**G_{LR} [MPa]**	**G_{LT} [MPa]**	**G_{RT} [MPa]**
	700	700	40
Poisson's ratio	**ν_{LR} [-]**	**ν_{LT} [-]**	**ν_{RT} [-]**
	0.015	0.038	0.558
Frictional properties	**$\mu_{parallel}$ [-]**	**$\mu_{perpendicular}$ [-]**	
	0.29	0.34	

6.2.4 Mesh

The mesh size, see Table 6.4, used in the model was the same as the determined size for model 3a in Section 6.1. The mesh for one beam in the stress-laminated deck is illustrated in Figure 6.6.

Table 6.4 Mesh size for model 3b in the three different directions.

Element type	Longitudinal, x	Transverse, y	Height, z
8 node solid, C3D8R	100 mm	95 mm	45 mm

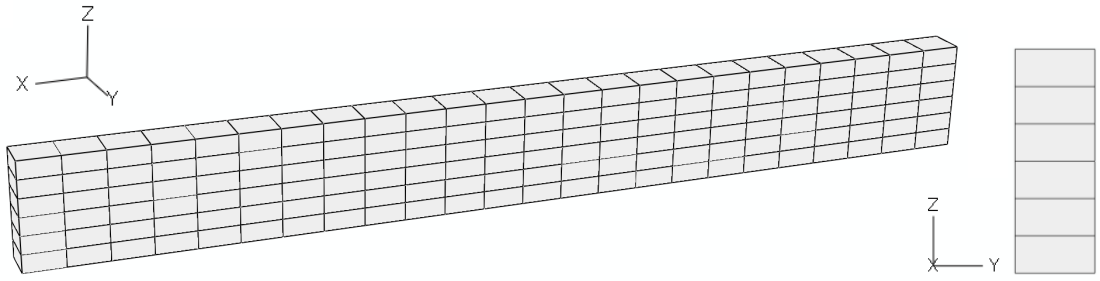

Figure 6.6 Mesh distribution on one beam in the stress-laminated deck.

6.3 Results

To determine which factor that influences the result from the finite element analysis, several analyses with changed variables were performed. The finite element results were compared to the test results from the full-scale test, which was taken out from several deformation sensors in the timber deck.

The placement of the different sensors, used in the full-scale test by SP Trätek, is showed in Figure 6.7. These sensors registered the vertical deformations on top of the timber deck while the deck was loaded, and this was also the points from where the finite element result was taken from. The numbering of the sensors starts from one at the loaded edge and increases towards the right side.

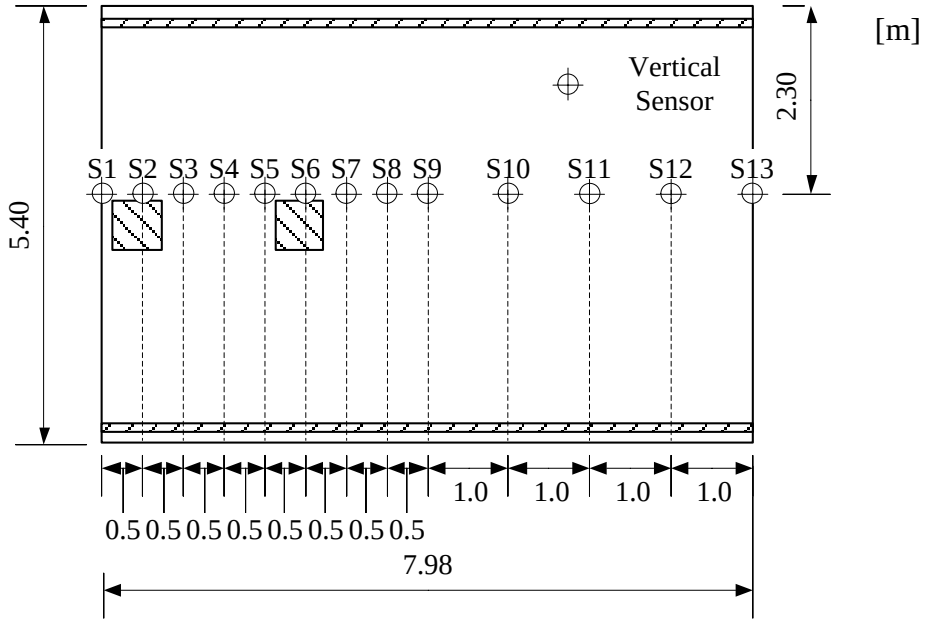

Figure 6.7 Sensors in the full-scale test by SP Trätek for measurement of vertical deformations.

In the work with model 3b different analyses and verifications were performed. A case called the standard case was determined as a starting point for most of the analyses. The standard case is defined with the previously determined settings in Section 6.2.

All the analyses started from the standard case properties, and was changed one each at a time according to Table 6.5. The results was analysed and compared to the global deflection profile in Figure 6.12 to Figure 6.18.

It is important to notice that for most of the analyses, when the standard case was used, the setting NLGEOM in ABAQUS was active. This make the analysis to take second order effects into account, i.e. taking into account the changed geometry in the incremental loading of the model. When large deformations are expected in the analysis the NLGEOM shall, according to the ABAQUS theory manual, be set as active. The setting NLGEOM is further discussed in Section 6.3.7.

Table 6.5 Test scheme for the variations of the material data for model 3b, bold text in the table denotes the standard case.

	Decreased	**Standard case**	Increased	Figure
Elastic slip [mm]				
	-	**0.1**	0.5 & 1.0	6.12 & 6.13
Stiffness [MPa]				
Longitudinal, E_L	11000	**12000**	13000	6.14
Transverse, E_T	300	**600**	900	6.15
Poisson's ratio [-]				
ν_{RT} [-]	**-**	**0.558**	0.700	6.16
Friction coefficient [-]				
Parallel, $\mu_{parallel}$	0.25	**0.29**	0.35	6.17
Perpendicular, $\mu_{perpendicular}$	0.30	**0.34**	0.40	6.18

6.3.1 Global deflection check

Model 3b consists of 84 glulam beams, modelled with symmetry boundary conditions in the longitudinal direction which represent the true geometry of the timber deck. There is an option to model with 42 beams and symmetry in both directions, i.e. longitudinal and transversal direction. However, it must be noted that symmetry boundary condition in the transverse direction is not fully correct for the edge load case because it represent a load on both edges.

An extra model was created with 42 beams to test the behaviour of a reduced number of beams. The properties were equal to the 84 beams model, i.e. the standard case defined in Table 6.3 and Table 6.5. In Figure 6.8 the deflection transverse the bridge deck for the different cases is showed and compared to the result from the full-scale test performed by SP Trätek. As showed the deflection from 0 m to 1.5 m towards the middle was similar but from 1.5 m to 4 m it differs.

This example shows that there is a possibility to model the timber deck with a reduced number of beams and still obtain a fairly good result. To reduce computational time, but with the cost of accuracy, the stress-laminated-timber deck can be modelled with a reduced number of beams. However, as the complete behaviour was studied in this thesis, the following analyses were performed with the 84 beams case, i.e. the standard case.

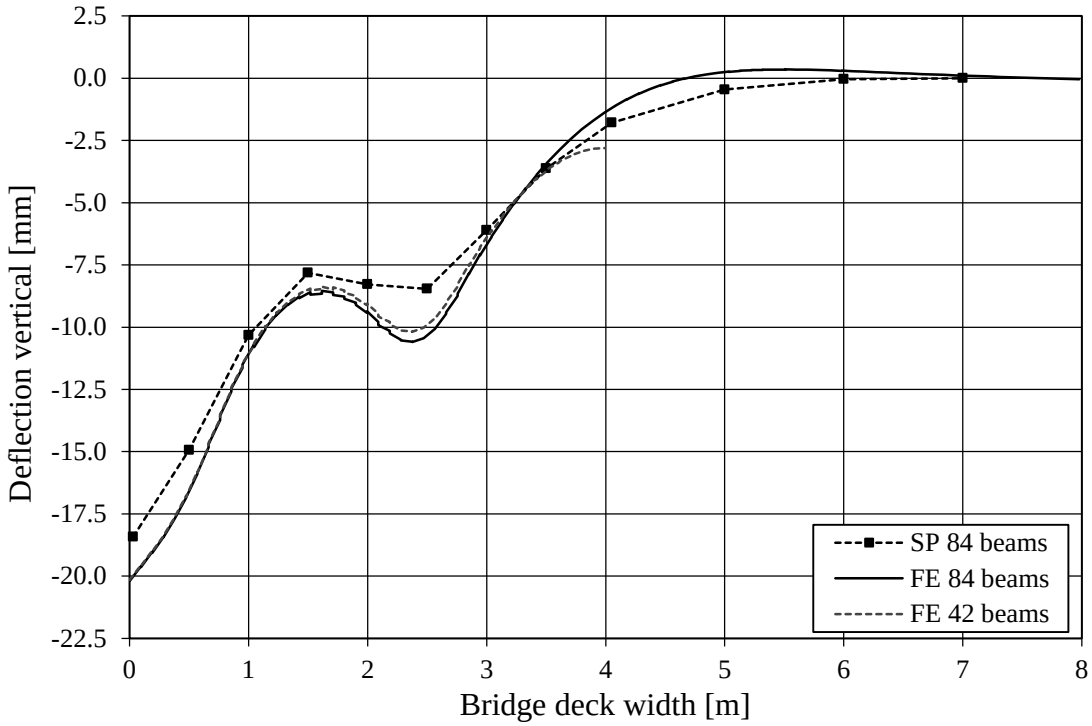

Figure 6.8 Deflection transverse the timber deck for different number of beams at a load of 300 kN and a pre-stress level of 0.6 MPa compared to the full-scale test performed by SP Trätek.

6.3.2 Linear vs. non-linear model

The finite element model describing model 3b have a non-linear geometry, i.e. each beam in the deck is modelled separately and put together with contact properties having frictional behaviour. However, there is a possibility to model the deck with a linear model, i.e. a homogenous plate.

The linear finite element model has the same properties as the 84 beams non-linear model except for the friction formulation. To obtain a model created by separate parts including contact to behave as a linear homogenous plate, the rough friction formulation can be used, see Section 2.4.6. The rough friction formulation uses a frictional coefficient which is defined as infinite high. However, the rough formulation must be set to not allow separation of the parts after contact, i.e. to not have a non-linear geometry.

In Figure 6.9 the difference in behaviour between a linear and a non-linear model at 600 kN load is showed compared to the result from the full-scale test performed by SP Trätek. As showed the difference was largest in the area under the loading, i.e. from 0 m to 3 m, where the vertical deformations generally was underestimated in the linear model.

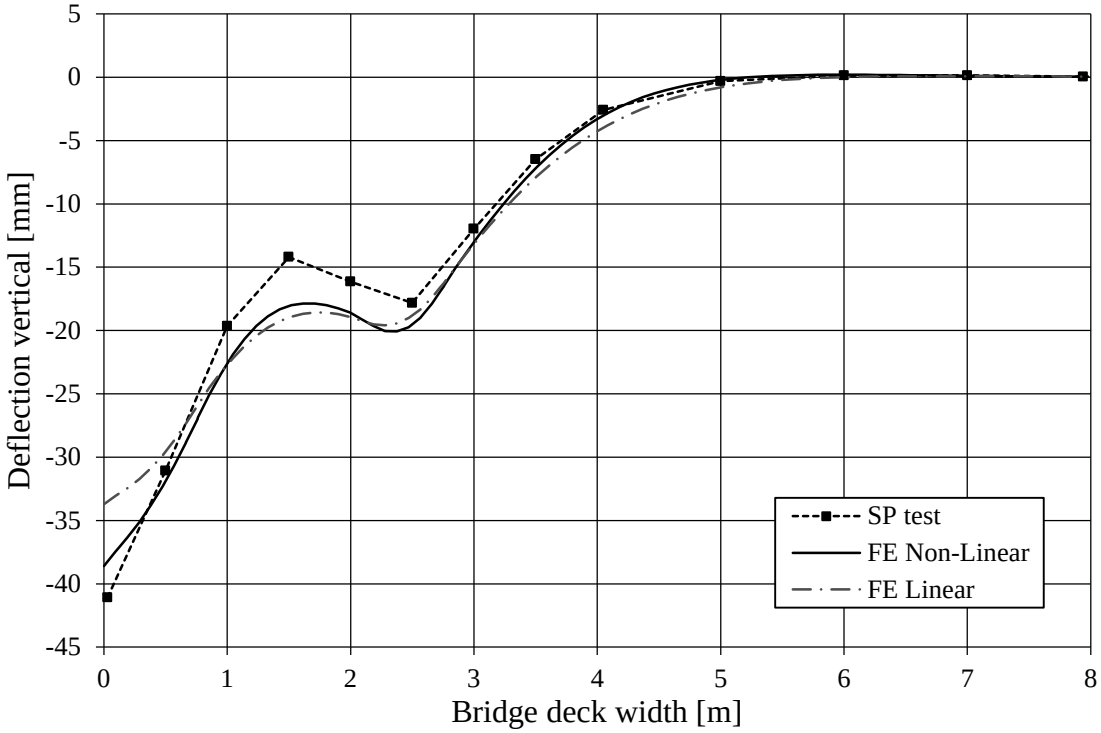

Figure 6.9 Deflection profile for linear vs. non-linear FE analysis at 600 kN compared to the full-scale test performed by SP Trätek.

In Figure 6.10 the deflection profile transverse the timber bridge deck, for the same loading case as in in Figure 6.9, is showed. One of the most interesting parts, when comparing a linear-and a non-linear analysis, is the area just under the loaded surfaces as it is most prone to interlaminar slip and opening between the beams.

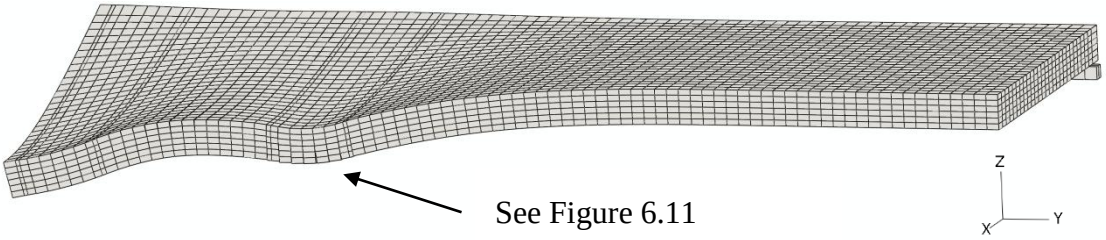

Figure 6.10 Deflection profile, shown with a magnification scale factor of 15, transverse the stress-laminated-timber deck at 600 kN with a non-linear analysis.

When a non-linear analysis is performed it is possible to notice if openings and interlaminar slip occurs, i.e. when a beam is moving next to another one. In the non-linear analysis this clearly occurs in these areas, see Figure 6.11a. When the analysis was performed with a linear model, though, these local effects are not possible to model, see Figure 6.11b. The importance of a non-linear model is clearly showed from this analysis.

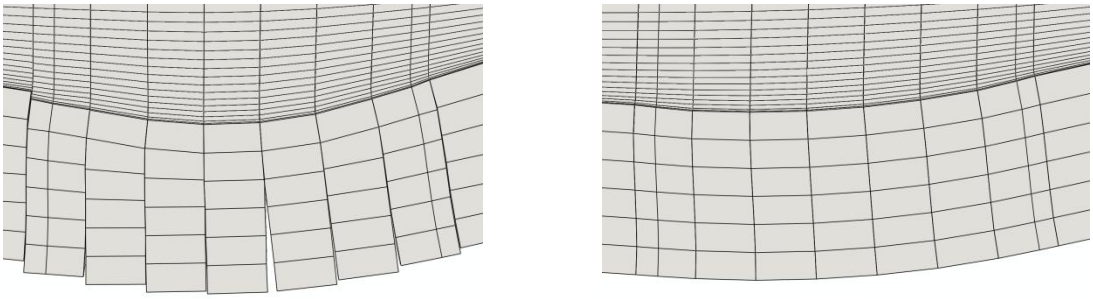

a) b)

Figure 6.11 a) Opening and interlaminar slip between the beams for non-linear analysis. b) Uniform deflection for linear analysis. Both figures are shown with a magnification scale factor of 15.

When the comparison of the results, between the linear and the non-linear analysis, was performed in more details it was noticed that the size of the elastic slip had impact on the vertical deflection already from the start of the analysis. When the self-weight was introduced to the model, i.e. at the very beginning of the analysis, it was expected that the vertical deflection would be exactly the same when using a linear or non-linear model. The difference was expected to come later, when the loading of the deck makes the geometry to be non-linear, i.e. when interlaminar slip and opening between the beams would occur. This phenomenon will be further presented in Section 6.3.7.

6.3.3 Elastic slip

From the evaluations of the first two models in this thesis, an appropriate distance of elastic slip was determined to be between 0.1 mm and 0.5 mm. A distance of 0.5 mm was set as starting point also for model 3. In Figure 6.12 and Figure 6.13 the effects on the deflection transverse the timber deck, at two different load levels, from higher and lower values of elastic slip distances are compared to the full-scale test performed by SP Trätek.

As showed in the figures a smaller elastic slip distance, down to 0.1 mm, represent the deflection shape obtained from full-scale test SP Trätek better, while a larger elastic slip distance makes it more inaccurate. The largest differences can be noticed directly under the load. From these observations the standard case for model 3b was determined to 0.1 mm and this setting was noted as important for the overall structural behaviour.

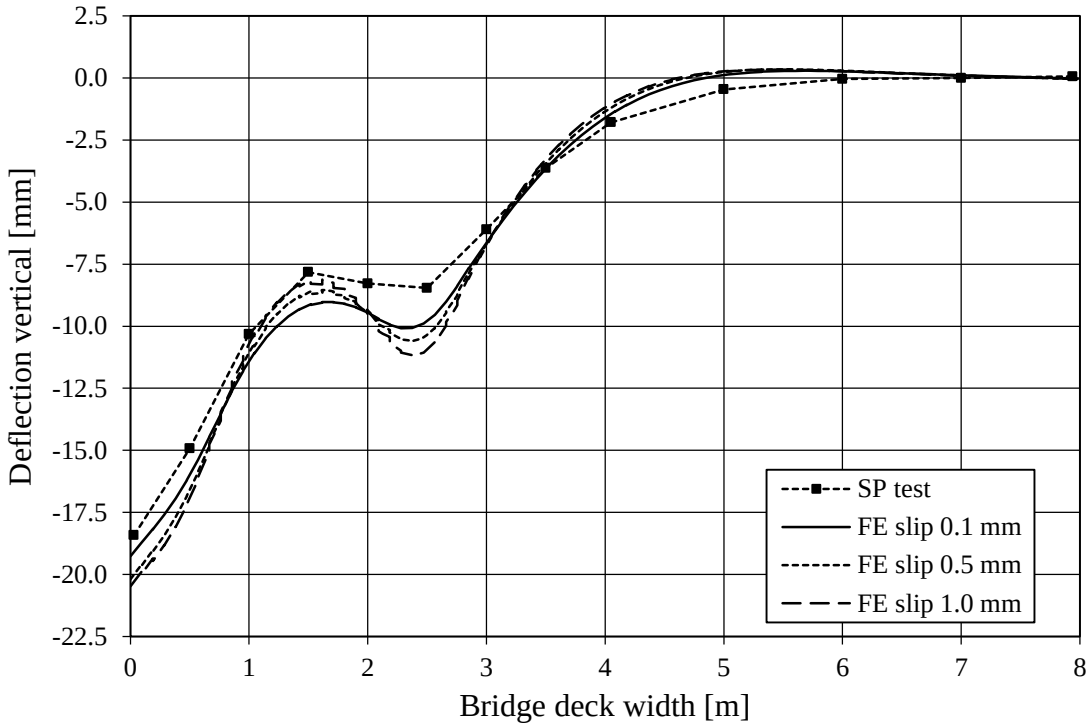

Figure 6.12 The effect from different elastic slip distance on the deflection at 300 kN transverse the timber deck compared to the full-scale test performed by SP Trätek.

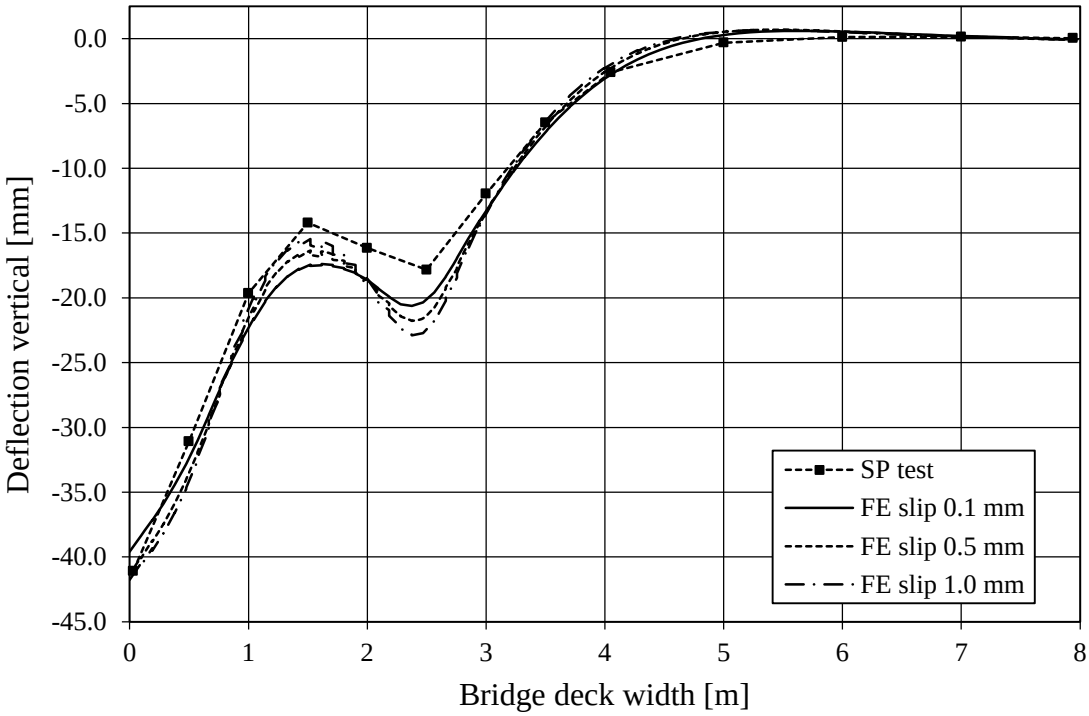

Figure 6.13 The effect from different elastic slip distance on the deflection at 600 kN transverse the timber deck compared to the full-scale test performed by SP Trätek.

6.3.4 Stiffness properties

The differences in the magnitude of the Young's modulus in the longitudinal direction are shown in Figure 6.14. The standard case was set to 12000 MPa. When increasing the stiffness to 13000 MPa the response of the deflection transverse the timber deck becomes more similar to the full-scale test. In the opposite way, when decreasing the stiffness to 11000 MPa the deflection increases. From this it can be concluded that the deflection under and close to the loaded area is affected by the magnitude of the bending stiffness.

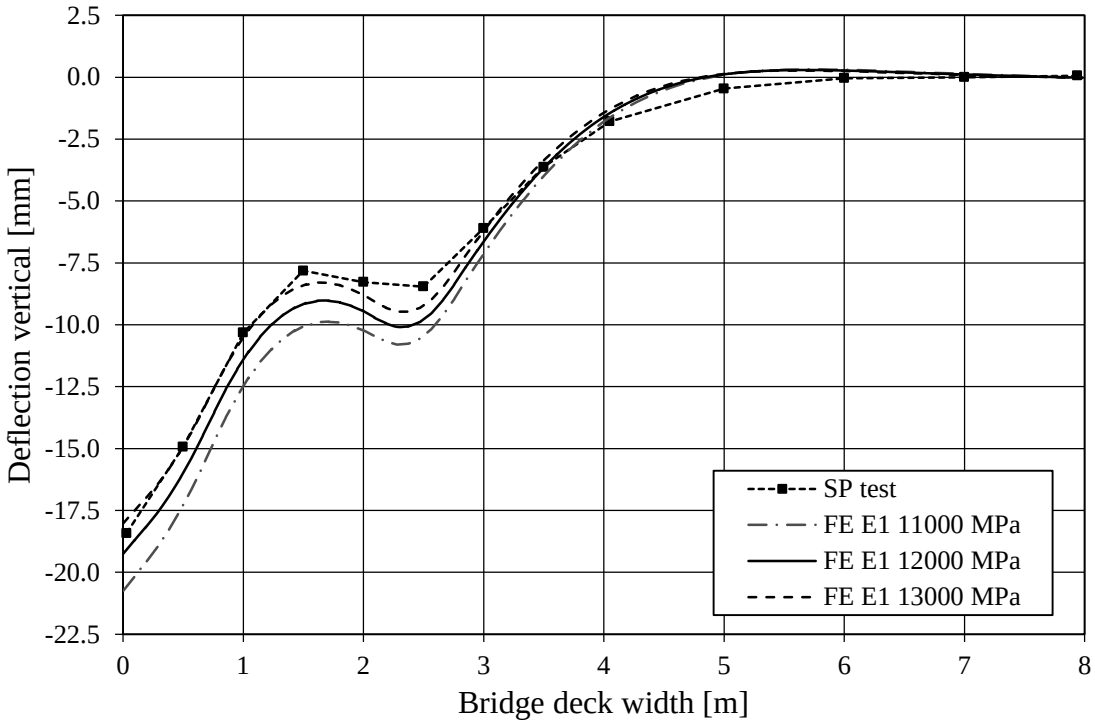

Figure 6.14 The effect from different longitudinal stiffness of the glulam beams, E1, on the deflection at 300 kN transverse the timber deck compared to the full-scale test performed by SP Trätek.

The differences in the magnitude of the Young's modulus in the transverse direction are shown in Figure 6.15. In the basic analysis case the transverse stiffness was set to 600 MPa. When increasing the stiffness to 900 MPa the magnitude of the deflection response transverse the timber deck becomes more similar to the full-scale test. In the opposite way, when decreasing the stiffness to 300 MPa, the deflection increases.

In the area between 1 m and 5 m the magnitude of the transverse stiffness is important because, as showed in Figure 6.15, the deflection tends to be negative, i.e. less deflection, when the stiffness is decreased. When increasing the transverse stiffness the load is distributed on more beams, hence the behaviour becomes more like a slab than a beam.

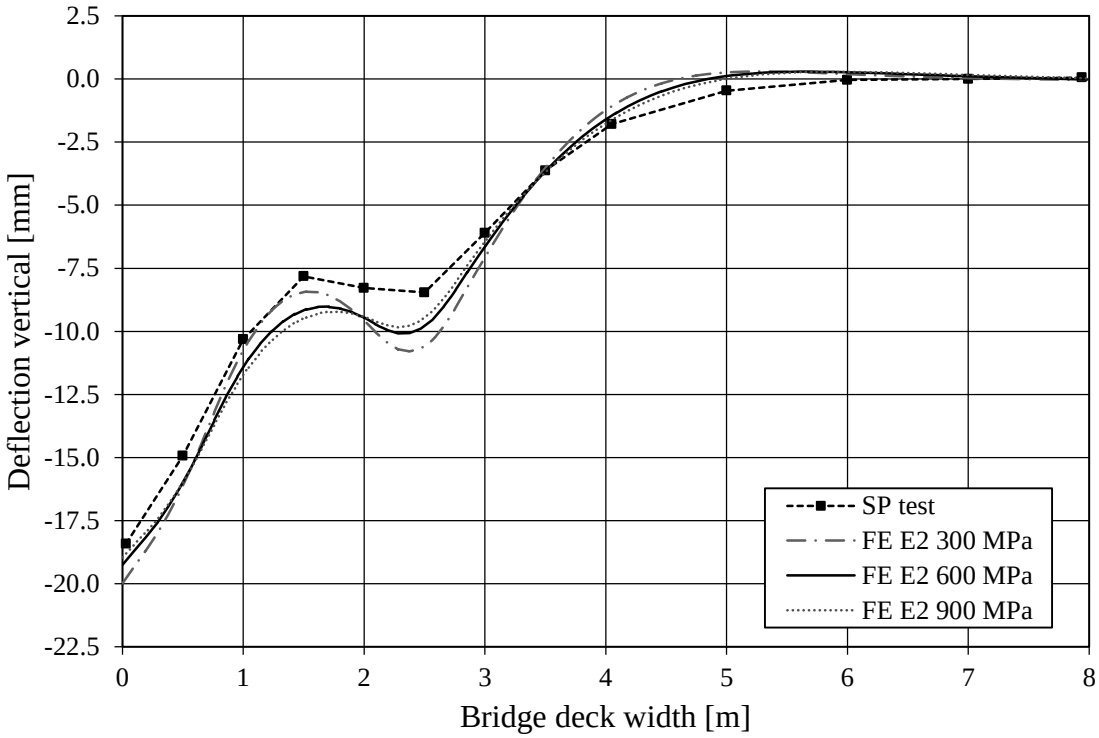

Figure 6.15 The effect from different transverse stiffness of the glulam beams, E2, on the deflection at 300 kN transverse the timber deck compared to the full-scale test performed by SP Trätek.

6.3.5 Lateral contraction

In Figure 6.16 the effect from higher coefficient of lateral contraction, i.e. Poisson's ratio, is shown. When increasing it from 0.558 to 0.7 it does not affect the deflection profile transverse the timber deck. This test concludes that Poisson's ratio is not very important when comparing the deflection transverse the timber decks hence no more analyses of this parameter are needed in this study.

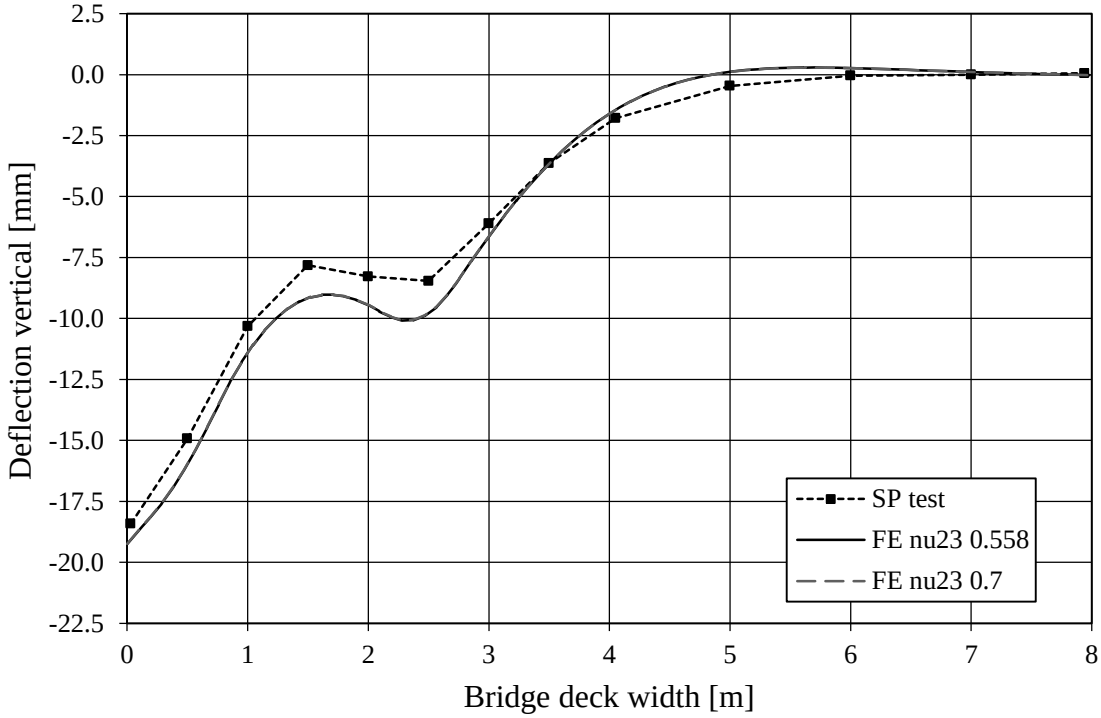

Figure 6.16 The effect from different Poisson's ratio for the glulam beams on the deflection at 300 kN transverse the timber deck compared to the full-scale test performed by SP Trätek.

6.3.6 Coefficient of friction

In Figure 6.17 and Figure 6.18 the response for different coefficient of friction is showed for a load of 300 kN and 600 kN. As showed, there was not a big difference when changing the coefficient of friction. In Figure 6.18 at 600 kN a slight difference was observed at the left edge of the bridge deck, i.e. directly below the load. At this position the finite element analysis underestimates the vertical deflection measured in the full-scale test performed by SP Trätek. This indicates that there was more local movement between the beams in this part of the stress-laminated deck in the full-scale test than in the finite element analysis.

However, the noticed effects on the vertical deflection of different friction coefficients was very small close to the mid span in the deck, i.e. in sensor 1 to 13 showed in Figure 6.7. This indicates that there was no large vertical slip, in this area of the stress-laminated deck, at this load levels in the finite element analysis.

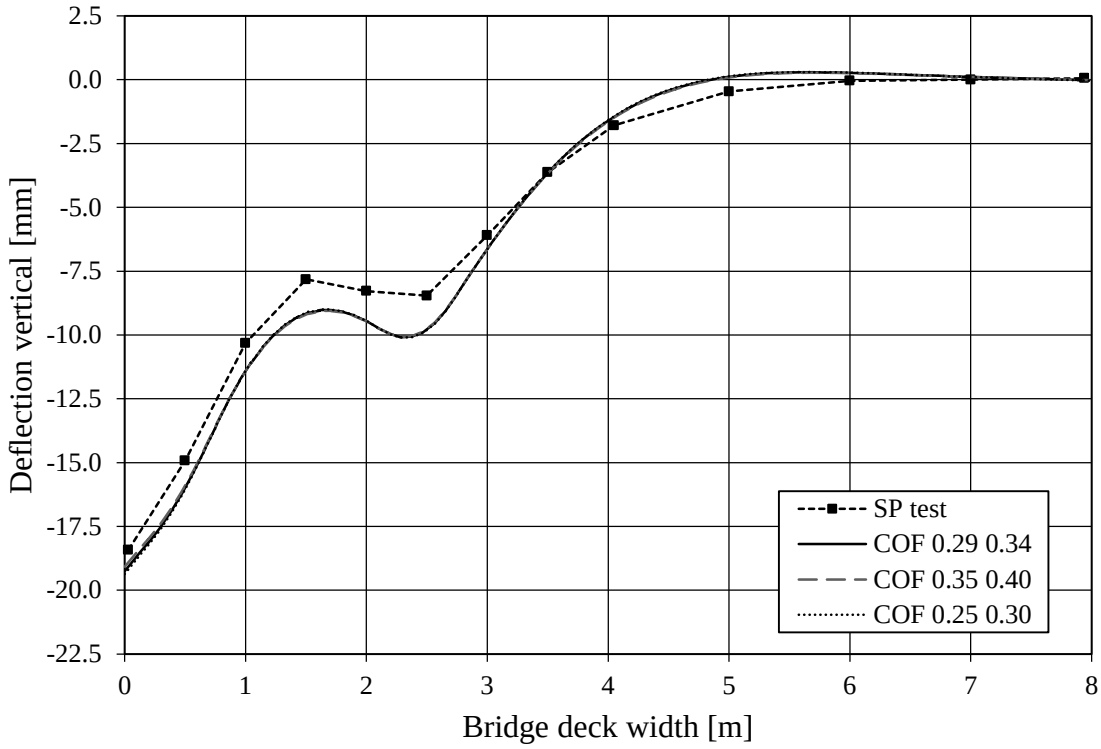

Figure 6.17 The effect from different coefficient of friction (COF) between the glulam beams on the deflection at 300 kN transverse the timber deck compared to the full-scale test performed by SP Trätek.

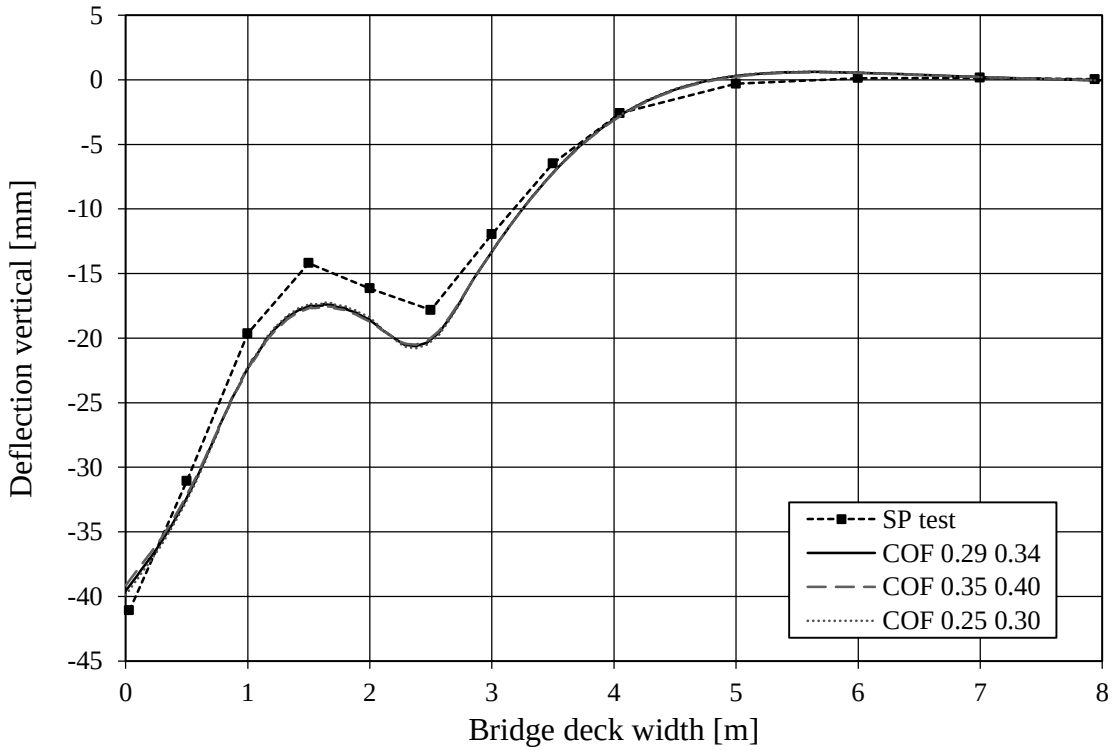

Figure 6.18 The effect from different coefficient of friction (COF) between the glulam beams on the deflection at 600 kN transverse the timber deck compared to the full-scale test performed by SP Trätek.

6.3.7 NLGEOM and elastic slip

The expected behaviour of the non-linear analysis was that the response should be linear up to a certain value and then become non-linear, i.e. when slip and opening between the beams should start to occur. The non-linear analysis was performed with an elastic slip distance of 0.1 mm, as defined for the standard case. However, a small difference in the response between the linear- and the non-linear analysis, with elastic slip 0.1 mm was observed already in beginning of the analysis, see Figure 6.19.

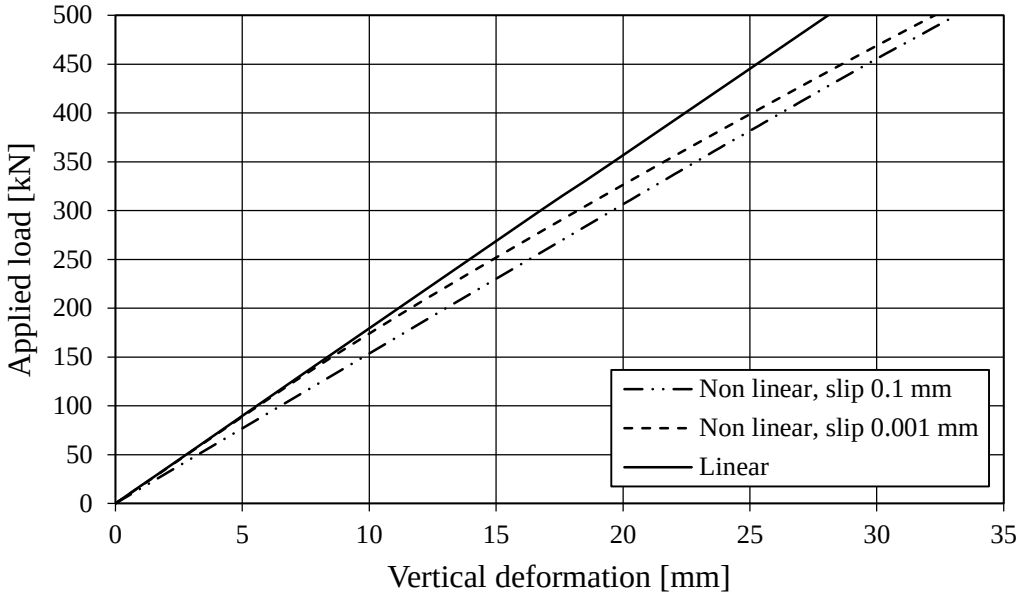

Figure 6.19 Load vs. deflection in sensor 1 for different elastic slip distance compared to the linear analysis.

When decreasing the elastic slip distance to 0.001 mm the result was similar to the linear analysis in the beginning. In Figure 6.20 the difference in response for different distance of elastic slip is showed in the very beginning of the analysis, i.e. when the self-weight is introduced in the model, and it is compared to the linear analysis.

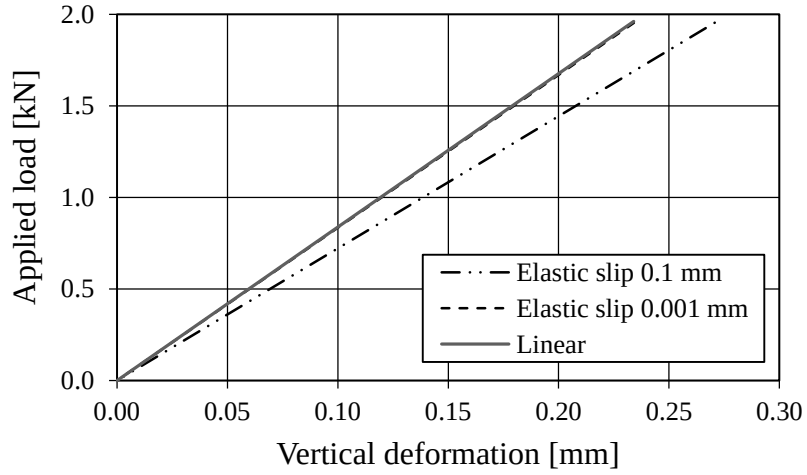

Figure 6.20 Load vs. deflection in sensor 1 when self-weight is applied for different elastic slip distance compared to the result from a linear analysis.

This observation gave some thoughts that the non-linear analysis of the stress-laminated-timber deck should instead be performed with a decreased elastic distance to be more similar to the linear one.

When trying to load the model with a load corresponding to the failure load in the SP Trätek full-scale test, i.e. 900 kN, some differences were noticed regarding the setting NLGEOM used in ABAQUS. The NLGEOM factor should, according to ABAQUS theory manual, be used to include second order effects in the analysis when one expects large deformations. When used the stiffness matrix is calculated using the current configuration i.e. using the current position of the nodes.

In Figure 6.21 the difference when using the NLGEOM factor or not is showed. When running the non-linear analysis without the NLGEOM setting the maximum load is 900 kN while when using the NLGEOM setting, the analysis interrupts at a load of approximately 500 kN due to problems with divergence. For the case, when NLGEOM is active, the response for increasing load differs somewhat. At loads larger than 300 kN the deformation increases, i.e. the response becomes less stiff.

It was hereby conclude that, it is not possible to use a very small slip and analyse the model for a higher load when the NLGEOM factor is set as active.

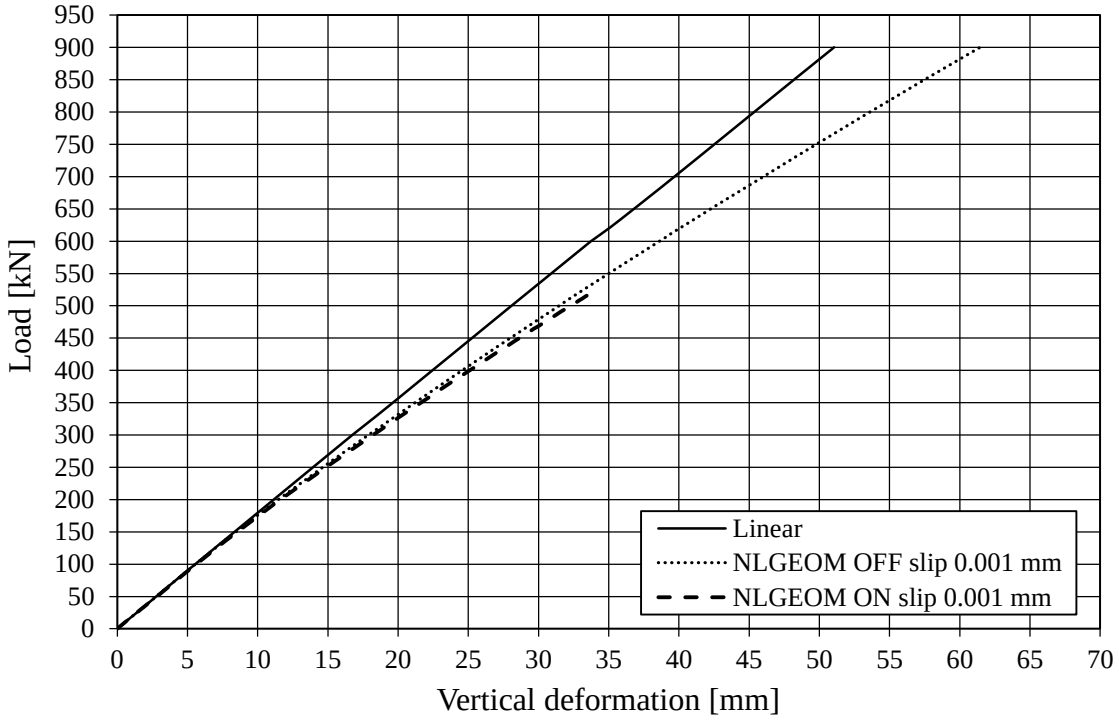

Figure 6.21 Load vs. deflection sensor 1 for NLGEOM factor on and off, for elastic slip fixed to 0.01 mm compared to the linear analysis.

In Figure 6.22 the result from the non-linear analysis, using an elastic slip of 0.1 mm, is showed for two different sensors, see Figure 6.7, in the stress-laminated deck. The result is showed for both the NLGEOM activated and deactivated. The result is compared to the full-scale test performed by SP Trätek.

As showed in the figure it was a very good match for sensor 1, i.e. at the edge of the deck when using the NLGEOM setting, while in sensor 2, i.e. 0.5 m from the edge, the comparison was not as good. In sensor 2 the result even indicates that, when using NLGEOM as deactivated the result is more accurate compared to the SP Trätek full-scale test.

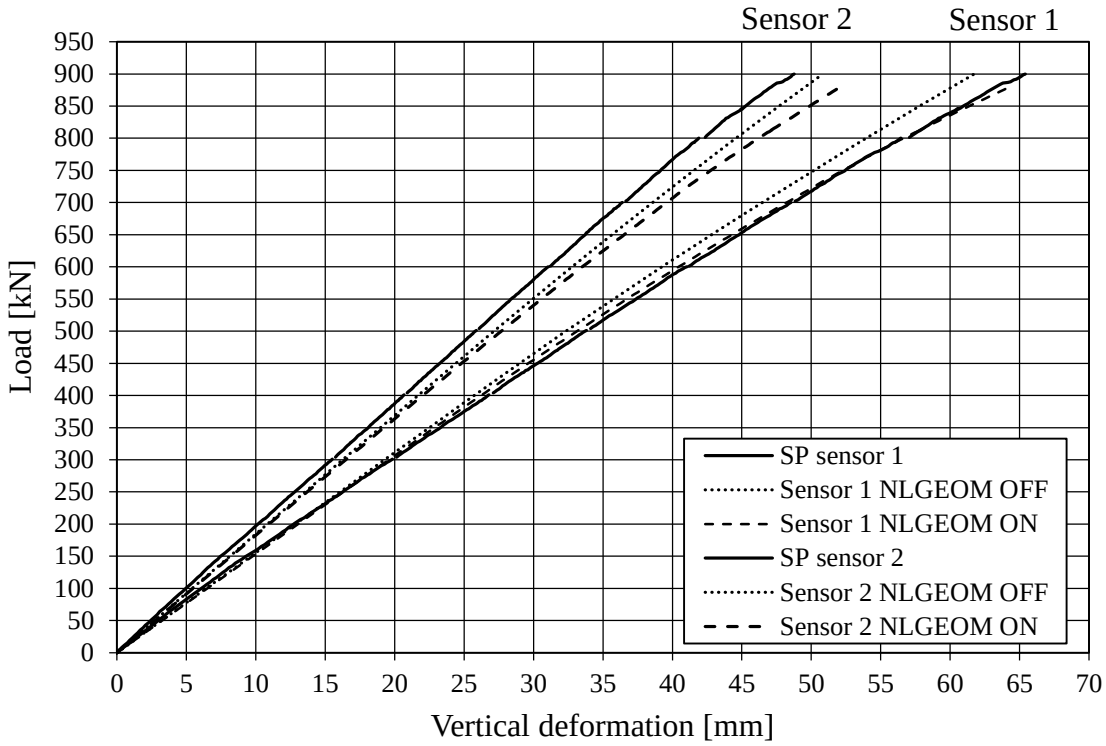

Figure 6.22 Load vs. deflection when NLGEOM is turned on or off with an elastic slip of 0.1 mm.

If the NLGEOM factor should be used in this type of analysis is not clear, there are both pros and cons with it as described in this section. If the solution will converge or not depends on if one uses the NLGEOM setting and the size of elastic slip distance. In Table 6.6 the different result for maximum load is showed. When comparing the response up to maximum obtained load, the behaviour also differs for where in the deck the comparison is performed as showed in Figure 6.22.

Table 6.6 Obtained results for model 3b for different settings.

Analysis type	NLGEOM	Elastic slip [mm]	Maximum load
Linear	NO	-	900 kN
Non-linear	YES	0.100	880 kN
Non-linear	NO	0.100	900 kN
Non-linear	YES	0.001	500 kN
Non-linear	NO	0.001	900 kN

7 Discussion

7.1 The three models

This section includes a discussion about the work that has been done in the previous chapters. First there is a discussion about the three models and then the models will be compared to see if they show the same behaviour.

The purpose with the first model was to gain knowledge of how to model friction in ABAQUS. There were a lot of different parameters that needed to be understood in order to obtain a model that worked properly. The most important parameters showed to be elastic slip, mesh size and time step. When these parameters was set to proper values it seemed possible to model the frictional behaviour in a reliable way that corresponded to the basic theory of friction.

The second model was analysed in the same manner as the first model, but with the difference that it was verified against experimental result. The verification showed that elastic slip still was an important parameter. The magnitude of the maximum obtained force is, as expected, determined by the frictional coefficient and the acting normal force. These parameters are not so difficult to decide, but the problem is still to determine the values of the parameters that decide the response towards maximum force, e.g. the size of elastic slip.

In the third model the aim was to analyse a model of a bridge deck with help of the knowledge gained in the first two models. The model was verified against a full-scale test of a stress-laminated-timber deck. To determine the need of a non-linear model, it was compared to a linear model, i.e. an orthotropic homogenous plate. In the full-scale test the response showed to be linear up to a certain load, i.e. before interlaminar slip occurred. To obtain the non-linear model that behaves linear up to a certain load, a smaller elastic slip had to be used. The result gives reason to discuss two theories.

- With a larger elastic slip the non-linear model is non-linear already from the start, i.e. it differs already before the slipping occurs for the linear model.
- With a smaller elastic slip the non-linear model is approximately linear up to the point where the first slip occur.

When comparing these theories with the full-scale test, see Figure 6.19 to Figure 6.22, the conclusion is that the value of the elastic slip should be somewhere in between. The problem with using a small elastic slip is that the model reaches divergence at a relatively early state when increasing the load.

7.2 Elastic slip

Here will follow a discussion about the elastic slip since it is a phenomenon that is difficult to handle and has been a mutual problem for all the finite element models in this thesis. The elastic slip is influenced by several parameters.

- **Time step**
  To be able to obtain the desired elastic slip a sufficiently small time step has to be used. If the time step is too large, the point where the sticking phase turns into slipping can be missed or wrongly estimated. A general approximation can be to use a time step that is smaller or equal to the elastic slip.

- **Mesh size**
  When using a finer mesh it is easier to catch the elastic slip and the point when sticking turns to slipping. This is due to the basis of the finite element method, i.e. the approximation is not as large with a finer mesh.

- **Young's modulus**
  To obtain the desired elastic slip between two parts in contact, the Young's modulus of the actual parts, has to be high enough not to get elastic deformation of the parts itself before slipping has occurred. In Figure 5.6 the analysis is made with the transverse stiffness which is considerably lower than the longitudinal stiffness that is used in Figure 5.5.

7.3 NLGEOM

The issue with NLGEOM is if it should be included during the analyses. If there are large deformations in the model it should be turned on to include the second order effects. In model one and two this is not a large problem because the effect of NLGEOM is neglected due to small deformations.

The important discussion should be about model three. Here the deformation is relatively large when the load is large. But when NLGEOM is turned on it is only possible to apply a load up to approximately 500 kN before the analysis reach divergence, i.e. crashes. If NLGEOM is turned off the analysis can be performed with greater load and still converge.

In Figure 6.22 a comparison is performed between two analyses with the same properties except that NLGEOM is used in one and not used in the other. The two different cases are verified against the full-scale test performed by SP Trätek. When comparing the results, it shows that it varies from where in the stress-laminated-timber deck the result is taken out from.

Another observation is that when NLGEOM is turned on, lateral torsional buckling occurs in the compressed part before divergence occurs, see Figure 7.1. These phenomena where not observed during the full-scale test, which hence indicates that something is wrong with the model when the NLGEOM is used. This issue can depend on a faulty size of the tolerance used, by default $10^{\wedge -6}$, in the analysis.

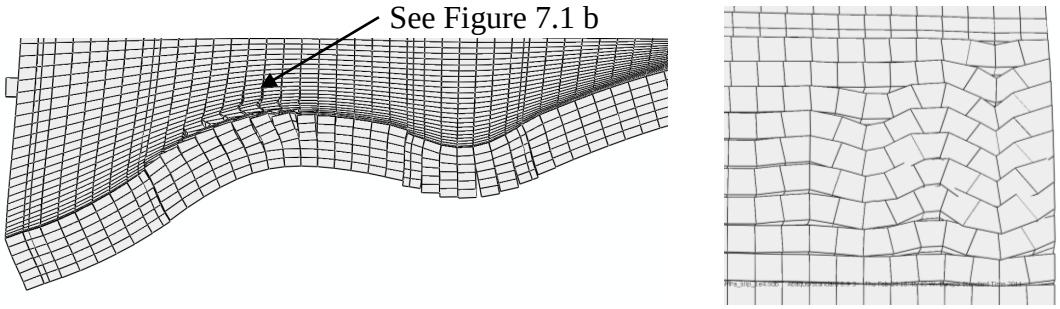

a) b)

Figure 7.1 *a) Compressed top in the deck is illustrated during loading at the edge b) lateral torsional buckling in the compressed part, shown with a magnification scale factor of 20.*

7.4 Friction coefficients

The third model was analysed with different values of the friction coefficient in the two directions. The result in Figure 6.17 and Figure 6.18 shows that, close to mid span of the timber deck, there were just small differences in deflection with different friction coefficient. A probable reason to why no difference was noticed can be either that the load was not large enough or too large to obtain slipping between the beams, i.e. the comparison was not performed under the correct load level. To find the needed force to create slipping between the beams this statement should be verified by comparing the magnitude of the actual shear force to the acting frictional force in detail.

The theory for the verification is shown in Figure 7.2. The frictional force, F_f is depending on the frictional coefficient, μ and the magnitude of the acting normal force, N. The acting normal force, N, is time dependent because it changes over time due to changed geometry, i.e. non-linear geometry. If the actual shear force is higher than the resisting frictional force, F_f, slipping will occur.

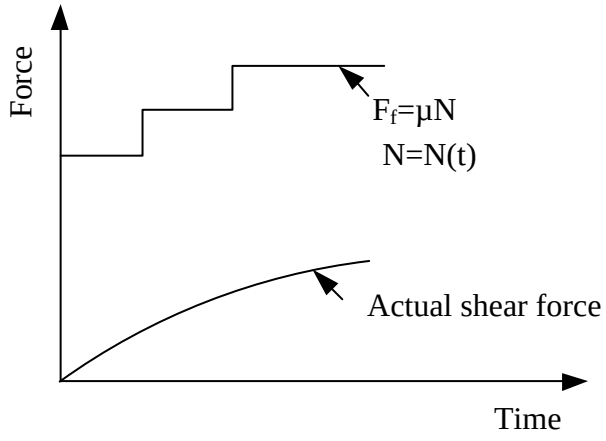

Figure 7.2 Comparison between the actual shear force and the frictional force, F_f needed to prevent slipping.

7.5 Load application

In model one and two the load is applied with deformation controlled load application, but in the third model it is applied as load controlled because it is more difficult to create a deformation controlled loading for this model when it should be verified at certain specific load levels. It is questionable if the third model should have had deformation controlled loading instead to increase the possibility of convergence in the analyses. Future testing regarding this has to be performed in order to know if this will reduce the convergence problems.

8 Conclusions

8.1 Modelling friction in ABAQUS

One of the purposes with this thesis was to learn how to model frictional behaviour in ABAQUS. The gained knowledge should be described in such matter it can be used for further studies and this purpose has been achieved.

- The most suitable frictional formulation was determined to be the penalty friction formulation.

- When using the penalty formulation, the size of the elastic slip distance is important. Elastic slip should be set as an absolute value, to be independent of the mesh size.

- The elastic slip requires a sufficiently large modulus of elasticity to show the expected response.

- The frictional force varies along a surface due to the effect of retarding forces which increase the normal force.

8.2 Application of the model on stress-laminated-timber decks

Another purpose was to apply the knowledge gained on how to model frictional behaviour on stress-laminated-timber decks. When applied it should be verified to experimental results. This purpose has been achieved and during the work the following important facts come up.

- Non-linear analysis is needed to obtain the real behaviour in the stress-laminated-timber deck when slip and opening between the beams occur, hence stress redistributions. A linear analysis underestimates the deflections and gives also faulty results regarding the stresses in the material because it does not take stress redistributions into account.

- The size of the elastic slip distance is important to produce the predicted linear or non-linear behaviour in a numerical finite element analysis. A too large elastic slip makes the model to behave non-linear to soon in an analysis compared to the real behaviour noticed in experimental tests.

8.3 Further investigations

- **Elastic slip**

  More studies have to be performed about the size of the elastic slip. More knowledge about what value should be used to obtain a correct behaviour when modelling stress-laminated-timber decks is needed.

- **NLGEOM**

  More analyses and evaluations have to be performed to be able to determine if NLGEOM should be included in the analyses of stress-laminated-timber decks. To prevent problems reaching convergence more studies and test of settings of the analysis has to be performed, e.g. time step and iteration method.

- **Load cycles**

  It is interesting to investigate if the created model of the stress-laminated-timber deck can handle load variations, similarly those performed in the full-scale test by SP Trätek. How the model will respond to unloading, i.e. if it will show the remaining deformations in a proper way is interesting to investigate.

- **Material properties**

  In the third model the same material properties are used for all the 84 beams. In the full-scale test by SP Trätek, and for timber in general, the material has a large scatter in its properties. Most interesting is to assign the same longitudinal stiffness properties, as measured in the full-scale test, to each beam in the model and study the effect on the non-linear behaviour.

9 References

ABAQUS theory manual 6.9 (2009): *ABAQUS theory manual, ABAQUS 6.9 documentation*, Software Manual, Dassault Systemes, 2009.

ABAQUS analysis user's manual 6.9 (2009): *ABAQUS analysis user's manual, ABAQUS 6.9 documentation*, Software Manual, Dassault Systemes, 2009.

Andersson E, Bergendahl J. (2009): *Experimental and Numerical Investigations on Stress Laminated Timber Bridges.* Master's Thesis. Department of Civil and Environmental Engineering, Division of Structural Engineering, Steel and Timber Structures, Chalmers University of Technology, Publication no. 2009:93, Göteborg, Sweden 2009.

Formolo S, Granström R (2007): *Compression perpendicular to the grain and reinforcement of pre-stressed timber deck-Theoretical studies, Laboratory tests and FE-analyses.* Master's Thesis. Department of Civil and Environmental Engineering, Division of Structural Engineering, Steel and Timber Structures, Chalmers University of Technology, Publication no. 2007:25, Göteborg, Sweden 2007.

Forest Products Laboratory. (2010): *Wood handbook- Wood as an Engineering Material.* Department of Agriculture, Forest Service, Forest Products Laboratory, Gen.Tech.Rep.FPL-GTR-190. Madison, Wisconsin 2010.

Forsberg G. (2010): *Friktionsprovning.* Report. SP Trätek Swedish Institute for Wood Technology Research, Rapport P805904-1, 2010.

Forsberg G. (2010): *Fullskaleförsök "Vägbro" på SP Trätek I Skellefteå,* Report. SP Trätek Swedish Institute for Wood Technology Research, Rapport P805094, 2010.

Kalbitzer T. (1999): *Stress-laminated-Timber Bridge Decks – Experiments regarding the Coefficient of Friction between Laminations.* Master's Thesis. Munich University of Technology, Germany, 1999.

Martinsons (2010): *Träbroguiden*. Guide. Martinsons Träbroar. Skellefteå 2010.

Pousette A. (2001): *Nordic Timber Bridge Project – Design values.* Report. SP Trätek Swedish Institute for Wood Technology Research, 2001.

Pousette A. (2008): *TRÄBROAR – konstruktion och dimensionering.* Handbook. SP Trätek Swedish Institute for Wood Technology Research, Rapport 2008:50, 2008.

Persson K. (2000): Micromechanical modelling of wood and fibre properties. Ph.D. Thesis. Department of Mechanics and Materials, Structural Mechanics, Lund University, ISRN LUTVDG/TVSM-00/1013-SE(1-223), Lund, Sweden.

Electronic sources:

Träguiden (2010): www.traguiden.se, 2010.